© 2017. Published by The Company of Biologists Ltd | Development (2017) 144, 2652-2662 doi:10.1242/dev.147751

RESEARCH ARTICLE

Convergence of signaling pathways underlying habenular formation and axonal outgrowth in zebrafish

Sara Roberson[1,2] and Marnie E. Halpern[1,2,*]

ABSTRACT

The habenular nuclei are a conserved integrating center in the vertebrate epithalamus, where they modulate diverse behaviors. Despite their importance, our understanding of habenular development is incomplete. Time-lapse imaging and fate mapping demonstrate that the dorsal habenulae (dHb) of zebrafish are derived from *dbx1b*-expressing (*dbx1b*$^+$) progenitors, which transition into *cxcr4b*-expressing neuronal precursors. The precursors give rise to differentiated neurons, the axons of which innervate the midbrain interpeduncular nucleus (IPN). Formation of the *dbx1b*$^+$ progenitor population relies on the activity of the Shh, Wnt and Fgf signaling pathways. Wnt and Fgf function additively to generate dHb progenitors. Surprisingly, Wnt signaling also negatively regulates *fgf8a*, confining expression to a discrete dorsal diencephalic domain. Moreover, the Wnt and Fgf pathways have opposing roles in transcriptional regulation of components of the Cxcr4-chemokine signaling pathway. The chemokine pathway, in turn, directs the posterior outgrowth of dHb efferents toward the IPN and, when disrupted, results in ectopic, anteriorly directed axonal projections. The results define a signaling network underlying the generation of dHb neurons and connectivity with their midbrain target.

KEY WORDS: Habenula, Interpeduncular nucleus, Shh, Wnt, Fgf, Chemokine

INTRODUCTION

The habenulo-interpeduncular (Hb-IPN) conduction system is a conserved feature of the vertebrate brain that modulates a variety of processes such as sleep, fear/anxiety, pain, learning, feeding, reproduction and reward (Sutherland, 1982; Benarroch, 2015; Namboodiri et al., 2016), and has been associated with mood disorders (Ranft et al., 2010; Savitz et al., 2011; Lawson et al., 2016) and addiction (Fowler et al., 2011; Baldwin et al., 2011). Recent attention has focused on the role of the Hb-IPN circuitry in nicotine dependence and withdrawal symptoms (Antolin-Fontes et al., 2015; Salas et al., 2009; Zhao-Shea et al., 2013; Pang et al., 2016) and the finding that, in zebrafish and other non-mammalian species, the bilaterally paired dorsal habenulae [dHb; equivalent to the medial habenulae (mHb) of mammals] (Aizawa et al., 2011) show prominent left-right differences in size, organization, molecular properties and connectivity (Braitenberg and Kemali, 1970; Concha and Wilson, 2001; Güntürkün and Ocklenburg, 2017; Duboué and Halpern, 2017). Although accumulating evidence demonstrates the importance and diverse functions of the habenular nuclei, our understanding of their development is incomplete.

The Hedgehog (Hh), Wnt and fibroblast growth factor (Fgf) signaling pathways have all been implicated in early habenular development. However, there are conflicting reports on whether Hh signaling antagonizes or promotes formation of the dHb (Chatterjee et al., 2014; Halluin et al., 2016). Mutations in the zebrafish *wntless* (*wls*) gene, which encodes a protein essential for Wnt secretion, or in the *fibroblast growth factor 8a* (*fgf8a*) gene, result in small dHb (Regan et al., 2009; Kuan et al., 2015). The small size of the dHb in *wls* and *fgf8a* mutant zebrafish is likely to be caused by a reduction in dHb progenitors (Kuan et al., 2015; Dean et al., 2014), which are characterized by their expression of the *developing brain homeobox 1b* (*dbx1b*) gene (Dean et al., 2014). The *Dbx1* gene was first identified as a marker of habenular progenitors in mice (Vue et al., 2007). In zebrafish, there are two homologs, *dbx1a* and *dbx1b*, but only *dbx1b* is expressed in dHb progenitors (Dean et al., 2014). Transcripts for the *chemokine (C-X-C) motif, receptor 4b* (*cxcr4b*) gene are also presumed to localize to habenular progenitors or newly born neurons (Roussigné et al., 2009; Halluin et al., 2016). However, the relationship between cells that express *dbx1b* and those that produce components of the Cxcr4-chemokine pathway is unresolved.

Through long-term lineage experiments, we demonstrate that *dbx1b*$^+$ progenitors give rise to all neurons in the dHb of adult zebrafish. During larval development, these progenitors undergo a transition during which they express both *dbx1b* and *cxcr4b*, then downregulate *dbx1b* and differentiate into *cxcr4b*-expressing neural precursors and, ultimately, dHb neurons. Hh, Wnt and Fgf signaling pathways are required for formation of *dbx1b*$^+$ progenitors. Analyses of zebrafish mutants indicate that Hh signaling is upstream or independent of Wnt signaling, and that Wnt activity restricts the domain of Fgf signaling. Wnt and Fgf signals are also necessary to delimit the expression domains of genes encoding Cxcr4-chemokine pathway components. We discovered that disruption of chemokine signaling perturbs the posteriorly directed outgrowth of dHb efferents, resulting in ectopic axonal projections. Thus, the action of multiple signaling pathways, through a complex regulatory network, promotes both the generation and connectivity of habenular neurons.

RESULTS

Progression of dHb development from *dbx1b*$^+$ progenitors to *cxcr4b*$^+$ neurons

Previous studies suggest that the *dbx1b* and *cxcr4b* genes are expressed by dHb progenitors (Dean et al., 2014; Roussigné et al., 2009; Halluin et al., 2016). A detailed analysis indicates that expression of the two genes is only partially overlapping at 35 h postfertilization (hpf) and 3 days postfertilization (dpf) (Fig. S1A-D). Thus, the precise relationship between the *dbx1b* and *cxcr4b* cell populations is unclear.

[1]Department of Biology, Johns Hopkins University, Baltimore, MD 21218, USA. [2]Department of Embryology, Carnegie Institution for Science, Baltimore, MD 21218, USA.

*Author for correspondence (halpern@carnegiescience.edu)

S.R., 0000-0002-6144-3521; M.E.H., 0000-0002-3634-9058

Received 1 December 2016; Accepted 7 June 2017

Development (2017) 144, 2652-2662 doi:10.1242/dev.147751

The identity of *dbx1b*$^{+}$ cells as progenitors of the dHb is well established on the basis of evidence from experiments in zebrafish (Dean et al., 2014) and the mouse homolog, *Dbx1* (Vue et al., 2007). In larval zebrafish, *dbx1b*$^{+}$ progenitors are located in a ventromedial location and give rise to neurons throughout the dHb (Dean et al., 2014). We confirmed these observations (Fig. S2A,B), and extended lineage tracing experiments to adults (Fig. S2C). Descendants of *dbx1b*$^{+}$ progenitors, distinguished by their mCherry-labeled nuclei, are found throughout the dHb of larvae and adults bearing *Tg(gng8:CAAX-GFP)*, which labels the membranes of dHb neurons and their efferent axons with GFP (deCarvalho et al., 2013).

Owing to the known role of Cxcr4b in cell migration (Lewellis and Knaut, 2012), we performed time-lapse imaging to determine whether *cxcr4b*$^{+}$ cells migrate to the developing dHb or whether *cxcr4b* expression is initiated *de novo* in *dbx1b*$^{+}$ progenitors. Images of *TgBAC(dbx1b:GFP)* and *TgBAC(cxcr4b:nls-tdTomato)* double-labeled embryos were captured every 15 min between 27 and 48 hpf (Fig. 1, Movie 1). At 27 hpf, GFP-labeled dHb progenitors are detected in wild-type (WT) embryos and, by 32 hpf, dTomato-positive nuclei appear within these GFP-labeled cells, demonstrating that *cxcr4b* expression initiates within pre-existing *dbx1b*$^{+}$ progenitors. We found no evidence for migration of dTomato-labeled cells into the presumptive habenular region.

In *wls* mutants, which produce fewer *dbx1b*$^{+}$ cells and have smaller dHb owing to reduced Wnt signaling (Kuan et al., 2015), there is a delay in the appearance of GFP-labeled and dTomato-labeled cells (35 and 40 hpf, respectively) (Fig. 1), and there are far fewer cells, consistent with a reduction in dHb progenitors. However, despite these defects, dTomato labeling is also only detected within the *dbx1b*$^{+}$ cells in *wls* mutants.

We next examined how *dbx1b* and *cxcr4b* expression changes during the course of habenular development (i.e. from 2 to 30 dpf) (Fig. 2). By 2 dpf, dTomato labeling is found in nuclei within the anterodorsal region of the dHb. By 3 dpf, GFP labeling becomes confined to a medial and ventral region of the developing dHb. The population of cells with dTomato-labeled nuclei increases in the dorsal and lateral regions, where GFP labeling is absent. However, a small number of colabeled cells are found at the border between the GFP and dTomato uniquely labeled domains. Restriction of GFP to an increasingly smaller ventromedial region, and the dorsolateral expansion of the dTomato-labeled cell population, continues over the course of several weeks.

Owing to persistence of dTomato labeling (Fig. S3A,B), we also examined the distribution of endogenous *cxcr4b* transcripts by fluorescent RNA *in situ* hybridization. Double labeling for *ELAV like neuron-specific RNA binding protein 3* (*elavl3*; formerly known as *HuC*) (Fig. 3A) or *anoctamin 2* (*ano2*) (Fig. 3B), which are expressed in mature dHb neurons (Kim et al., 1996; deCarvalho et al., 2014), indicates that *cxcr4b* transcription is rapidly terminated as dHb neurons differentiate. The results suggest that *dbx1b*$^{+}$ progenitors undergo a transition to *cxcr4b*$^{+}$ neural precursors, which then give rise to differentiated neurons.

Hedgehog signaling acts upstream or independent of Wnt signaling to specify dHb progenitors

Previously, Sonic hedgehog (Shh) signaling from the zona limitans interthalamica (ZLI) was found to be essential for formation of the dHb, as mutants for the Shh receptor Smoothened (Smo) lack *cxcr4b* expression in this region of the brain (Halluin et al., 2016) (Fig. 4A,A′). We find that expression of *dbx1b* is also absent in *smo* homozygous mutants (Fig. 4B-C′), indicative of the loss of dHb progenitors. Previously, mutations in the *wls* gene, which encodes a protein essential for secretion of Wnt proteins, were also found to reduce the dHb progenitor population (Kuan et al., 2015). To examine the relationship between Shh and Wnt signaling in dHb development, we assessed expression of *sonic hedgehog a* (*shha*) and the Hh-responsive gene *patched 1* (*ptch1*) in the ZLI of *wls* mutants. Expression of both genes appeared indistinguishable from that of WT siblings (Fig. 4D-G′), suggesting that Shh acts upstream or independently of Wnt signaling in the specification of dHb progenitors.

Diencephalic domain of Fgf signaling is restricted by Wnt signaling

Reduction of Fgf signaling using chemical inhibitors, or in *fgf8a* homozygous mutants, also results in fewer *dbx1b*-expressing

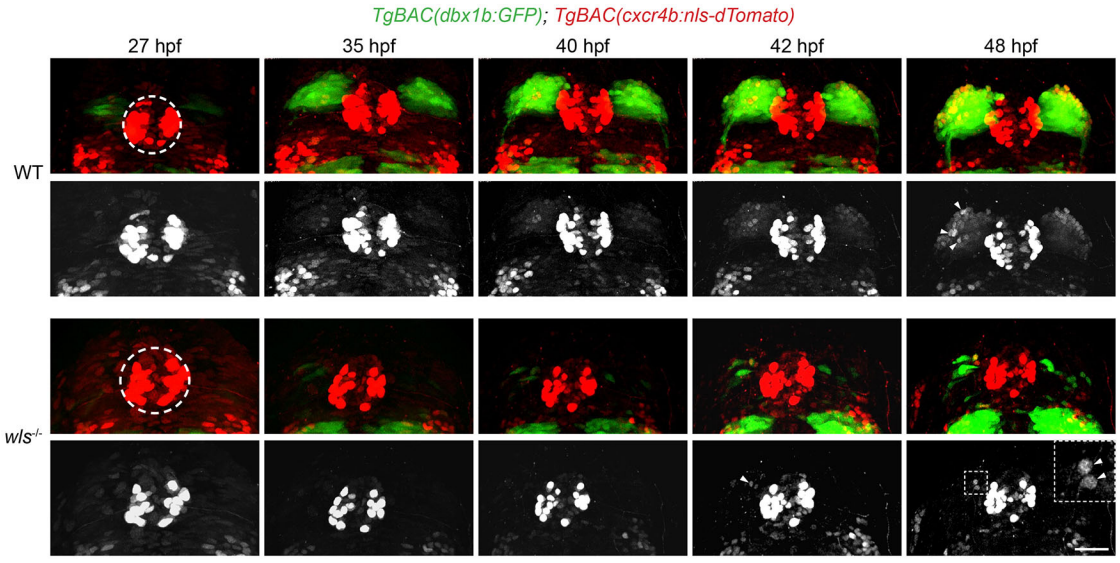

Fig. 1. Live imaging of *dbx1b*$^{+}$ and *cxcr4b*$^{+}$ populations. Live imaging of WT and *wls* mutant *TgBAC(dbx1b:GFP)* and *TgBAC(cxcr4b:nls-dTomato)* double-labeled embryos between 27 and 48 hpf (Movie 1). Black and white images are of dTomato-labeled nuclei alone. dTomato-labeled nuclei are found in the pineal anlage (dashed circle) and, over time, in cells arising within the developing dHb (arrowheads and inset). Scale bar: 30 µm (11 µm for inset).

Development (2017) 144, 2652-2662 doi:10.1242/dev.147751

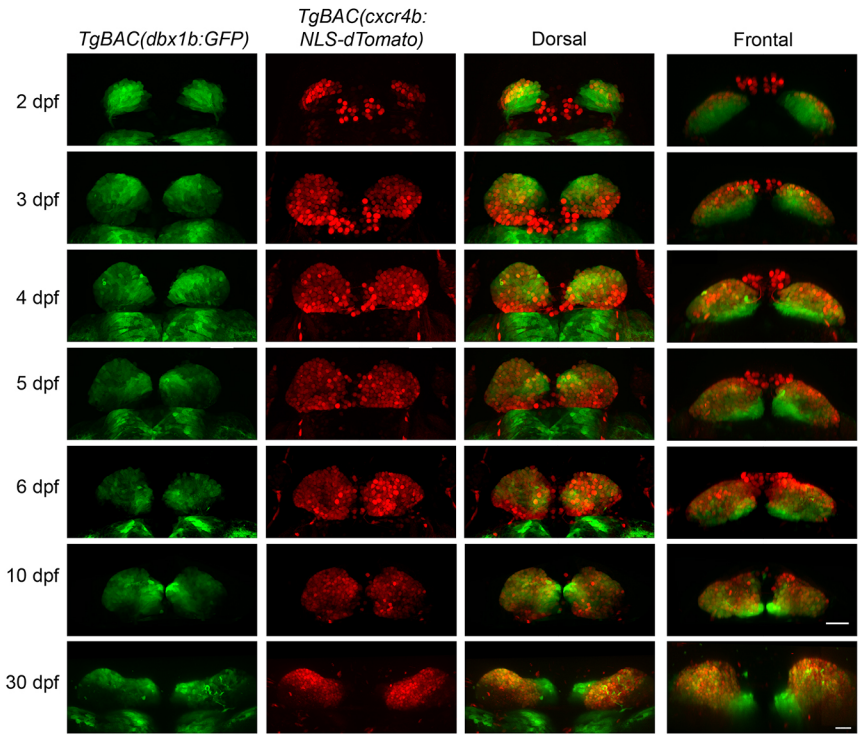

Fig. 2. Temporal switch in *dbx1b* and *cxcr4b* expression in the developing dHb. Relative positions of *dbx1b*$^{+}$ and *cxcr4b*$^{+}$ cell populations revealed by *TgBAC(dbx1b:GFP)* and *TgBAC(cxcr4b:nls-dTomato)* labeling, respectively, between 2 and 30 dpf. Merged images are shown in dorsal and frontal views. Scale bars: 30 µm.

progenitors (Dean et al., 2014) and small habenulae (Regan et al., 2009). Therefore, the reduced progenitor population observed in *wls* mutants could be caused by a lack of Fgf signaling. In WT embryos, expression of *fgf8a* is limited to cells just anterior of the developing dHb (Fig. 5A-C), within a region 28.9±1.8 µM long and 95.0 µM± 5.3 µM wide (n=7). However, rather than being lost or smaller, the *fgf8a* domain is expanded posteriorly (2.2-fold) and medially (1.4-fold) in *wls* mutants (n=7) (Fig. 5A′-C′, Table 1, Fig. S4A). A similar enlargement of the *fgf8a* domain is seen after heat shock-induced overexpression of the Wnt signaling inhibitor Dickkopf 1 (Dkk1) in 24 hpf *Tg(hsp70:dkk1-GFP)* embryos (Fig. 5D,D′). The result of expanded *fgf8a* expression in *wls* mutants is increased Fgf signaling, as evidenced by a corresponding expansion in the expression domains of Fgf-responsive genes, such as *dusp6* and *etv5b* (Fig. 5, Table 1, Fig. S4B,C). These findings indicate that, surprisingly, the reduction of dHb progenitors in *wls* mutants is not the result of decreased Fgf signaling. Instead, Wnt signaling normally acts to restrict the spatial extent of Fgf signaling in the dorsal diencephalon.

Given that Wnt and Fgf signaling are both important for the formation of *dbx1b*$^{+}$ dHb progenitors, we explored the epistatic relationship between these pathways. Transcripts for *dbx1b* are reduced in the dorsal diencephalon of *wls* and *fgf8a* single mutants compared to WT siblings. However, mutants doubly homozygous for *wls* and *fgf8a* completely lack *dbx1b* expression in this region and fail to form dHb (Fig. 5I-L and data not shown). Treatment of *wls* homozygous mutants with the Fgf receptor inhibitor SU5042 produces a similar phenotype, reducing *dbx1b*-expressing progenitors in a dose-dependent manner (Fig. S5). Thus, Wnt and Fgf signaling act in an additive manner to generate dHb progenitors.

Opposing roles for Wnt and Fgf signaling in regulating the Crxc4b-chemokine pathway

In addition to their role in the formation of dHb progenitors, Wnt and Fgf signaling are necessary for proper expression of Cxcr4-chemokine pathway components. This pathway includes Chemokine (C-X-C) motif ligand 12 (Cxcl12; formerly known as Stromal cell-derived factor-1 or Sdf1), which binds to the Cxcr4 receptor and the Atypical

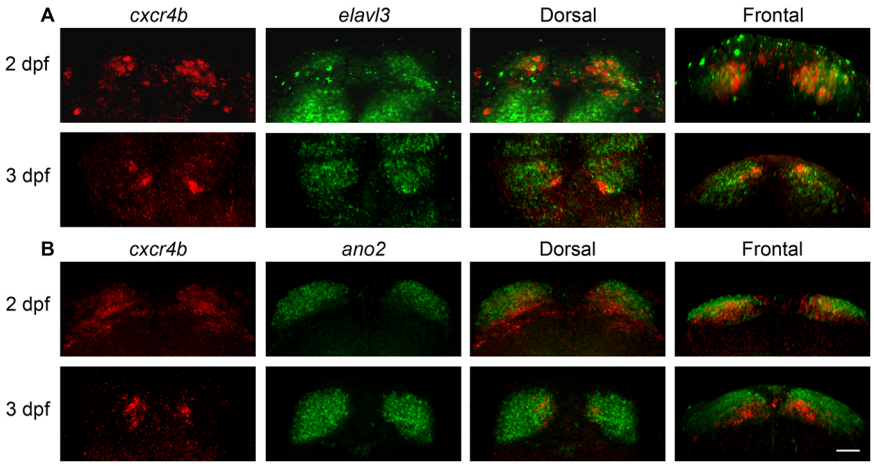

Fig. 3. Ventromedial position of *cxcr4b*-expressing cells relative to dHb neurons. Fluorescence *in situ* hybridization in 2 and 3 dpf larvae for transcripts of *cxcr4b* and (A) the pan-neuronal gene *elavl3* or (B) *ano2*, a marker of dHb neurons. The left three columns of images are corresponding dorsal views; the rightmost column shows frontal views. Scale bar: 30 µm.

Development (2017) 144, 2652-2662 doi:10.1242/dev.147751

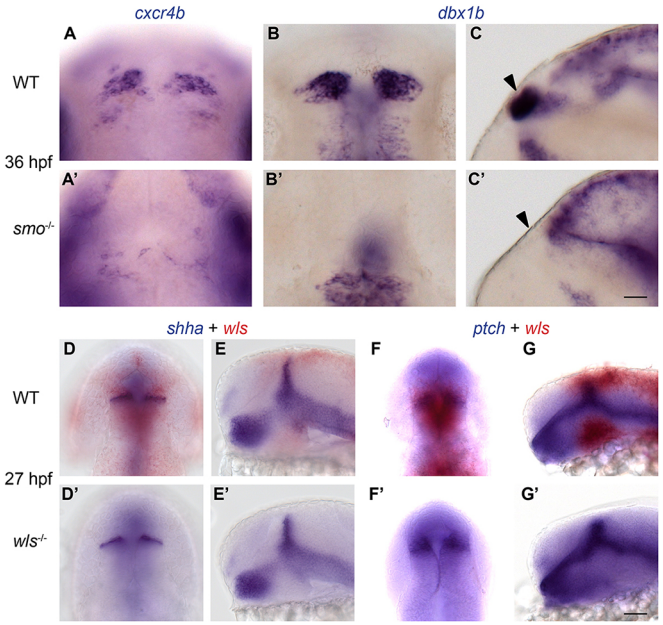

Fig. 4. Specification of *dbx1b*$^{+}$ dHb progenitors requires Shh signaling upstream of or parallel to Wnt signaling. At 36 hpf, (A,A′) *cxcr4b* and (B-C′) *dbx1b* transcripts are found in the developing dHb of (A,B,C) WT embryos, but not in the corresponding diencephalic region of (A′,B′,C′) *smo* mutants (arrowheads). Expression of (D-E′) *shha* and (F-G′) *ptch1* is comparable in (D,E,F,G) WT embryos and (D′,E′,F′,G′) *wls* mutants. Sibling WT and homozygous *wls* mutant embryos are distinguished by the presence or absence of *wls* transcripts (Kuan et al., 2015). Dorsal (A-B′,D,D′,F,F′) and lateral (C,C′,E,E′,G,G′) views are shown. Scale bars: 30 µm.

chemokine receptor 3 (Ackr3; formerly known as Chemokine receptor 7 or Cxcr7). Cxcr4 is the signaling receptor, whereas Ackr3 (the Ackr3b homolog) sequesters excess Cxcl12 to establish a local gradient (Dambly-Chaudiere et al., 2007; Lewellis and Knaut, 2012; Miyasaka et al., 2007; Boldajipour et al., 2008). Zebrafish have two Ackr3 and Cxcl12 homologs (a and b). At 35 hpf, *cxcl12a* transcripts are found in cells posterior to the *dbx1b*$^{+}$ developing habenulae (Fig. 6A-C), whereas *cxcl12b* is expressed in cells surrounding the habenular region, at higher levels anterior to the region and at lower levels posterior to it (Fig. 6D-F, Fig. S6A). Cells expressing *ackr3b* lie anterior to the *cxcl12b*$^{+}$ (Fig. S6B) and *dbx1b*$^{+}$ (Fig. S6C) populations, as well as in the midline between the developing dHb.

Disruption of Wnt or Fgf signaling significantly expands the expression patterns of *cxcl12b* and *ackr3b*. In *wls* mutants, *cxcl12b* is ectopically transcribed within the developing habenulae and at high levels both anteriorly and posteriorly [3-fold increase along the anterior-posterior (A-P) axis, Fig. 6G-H′, Table 1, Fig. S4D]. By contrast, *cxcl12a* transcripts appear unaffected (Fig. S3D). In *wls* mutants, midline expression of *ackr3b* also extends more laterally (2-fold wider) and posteriorly (1.9-fold longer) (Fig. 6I-J′, Table 1, Fig. S4E).

The enlarged *cxcl12b* and *ackr3b* expression domains (Fig. 6G-J′) resemble the expanded *fgf8a* expression observed in *wls* mutants (Fig. 5A-C′), suggesting that Fgf8a positively regulates expression of these chemokine pathway members. Consistent with this, the *cxcl12b* domain in the dorsal diencephalon in *fgf8a* homozygous mutants is almost half the size of the WT domain at 35 hpf (Fig. 6K-L′, Table 1, Fig. S4). Expression of *ackr3b* is also affected but to a lesser degree (Fig. 6M-N′, Table 1, Fig. S4). In *wls;fgf8a* double mutants (Fig. 6O-R), or in *wls* mutants treated with SU5042 (Fig. 6S-U′), the domain of *cxcl12b* expression is reduced relative to *wls* homozygous mutants and becomes more similar in size to the WT pattern (Table 1, Fig. S4D). Taken together, the results demonstrate that Fgf and Wnt signaling act antagonistically to define the expression domains of these members of the chemokine signaling pathway.

Cxcr4b-chemokine pathway is necessary for directional outgrowth of dHb axons

The function of the Cxcr4b-chemokine pathway in the developing dHb is unknown. Chemokine signaling is known to mediate cell cohesion and migration (Miyasaka et al., 2007; Palevitch et al., 2010; Aman and Piotrowski, 2008); however, the size and

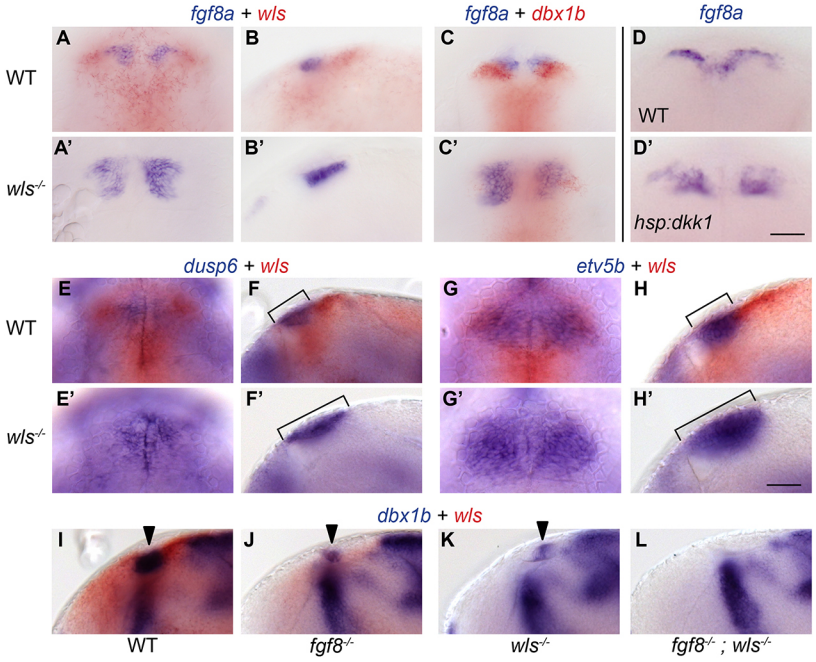

Fig. 5. Wnt signaling defines the domain of Fgf signaling in the dorsal diencephalon. (A-C′) At 35 hpf, the domain of *fgf8a* expression just rostral to the developing dHb is expanded in *wls* mutants. (D,D′) Inhibition of Wnt signaling at 36 hpf by heat shock activation of *Tg(hsp70:dkk1-GFP)* also expands *fgf8a* expression at 48 hpf. (E-H′) The expression domains of (E,F) *dusp6* and (G,H) *etv5b*, two targets of Fgf signaling, are enlarged in (E′,F′,G′,H′) *wls* mutants (compare brackets). (I-L) Expression of *dbx1b* (arrowheads) in the (I) WT dorsal diencephalon is reduced in (J) *fgf8a* and (K) *wls* mutants, and absent in (L) *fgf8a;wls* double mutants. Dorsal (A,C,D,E,G) and lateral (B,F,H,I-L) views are shown. Refer to Table 1 for numerical values. Sibling WT and homozygous *wls* mutant embryos were distinguished by the presence or absence of *wls* transcripts (Kuan et al., 2015). Scale bars: 50 µm.

Development (2017) 144, 2652-2662 doi:10.1242/dev.147751

Table 1. Spatial patterns of gene expression in WT and mutant dorsal diencephalon

		Gene expression domain (μm)								
		fgf8a		*etv5b*		*dusp6*		*cxcl12b*	*ackr3b*	
Genotype	Number quantified	A-P	M-L	A-P	M-L	A-P	M-L	A-P	A-P	M-L
wls$^{-/-}$	7, 9, 9, 12, 7	64.4±1.8	134.6±6.3	98.9±5.9	184.6±6.2	87.8±4.0	121.9±6	57.8±1.8	41.9±3.7	97.8±8.1
WT siblings	7, 11, 8, 16, 8	28.9±1.8	95±5.3	71.8±2.8	161±8.1	58.2±2.7	94.6±3.1	18.3±1.5	25.9±1.0	50.2±2.8
fgf8a$^{-/-}$	9, 12	–	–	–	–	–	–	9.1±1.4	22.3±1.8*	31.8±2.5
WT siblings	11, 7	–	–	–	–	–	–	18.0±3.1	23.8±2.3	51.3±1.8
wls$^{-/-}$;*fgf8a*$^{-/-}$	6	–	–	–	–	–	–	9.7±0.83‡	–	–
WT siblings	9	–	–	–	–	–	–	12.1±1.4	–	–

Measurements (μm) were taken along the anterior-posterior (A-P) and medial-lateral (M-L) axes for gene expression domains in the dorsal diencephalon at 35 hpf. Numbers quantified correspond with the order of the indicated genes from left to right. Significant differences were found between *wls* and WT for all expression domains examined (P<0.05).

*Homozygous *fgf8a* mutants are significantly different from WT siblings, with the exception of the *ackr3b* domain along the A-P axis (P=0.61).

‡A significant difference was not found between the *cxcl12b* expression domain in *wls;fgf8a* double mutants and their WT siblings (P=0.17).

morphology of the dHb appear normal in *cxcr4b* homozygous mutants (Fig. 7A,B and data not shown). Because Cxcr4-related receptors are also involved in axonal outgrowth and pathfinding by diverse neuronal types (Li et al., 2005; Miyasaka et al., 2007; Chalasani et al., 2003a,b; Lieberam et al., 2005), we examined the projections of dHb neurons.

As visualized by *Tg(gng8:CAAX-GFP)* labeling (Fig. 7A), axons of dHb neurons typically emerge at a lateral posterior position and fasciculate in the prominent bilateral fiber bundles of the fasciculus retroflexus (FR), which extend posteriorly to the midbrain IPN. We found that the majority of *cxcr4b* mutants have defective dHb axonal projections (Fig. 7B,E). Axonal phenotypes fall into three classes: in Class I larvae, the dHb-IPN projection is similar to WT; Class II larvae exhibit correctly directed axons that extend posteriorly, as well as ectopic anteriorly projecting axons; in Class III larvae, axons from the left and right dHb merge to form a thick bundle that extends anteriorly along the midline. In contrast to their WT or heterozygous siblings that predominantly showed the Class I phenotype (97.6%; n=41), most homozygous *cxcr4b* mutants displayed either Class II (48.6%) or Class III (45.7%) phenotypes (n=35). Similar defects were observed upon loss of the chemokine ligand Cxcl12a (Class II 66.6% and Class III 13.3%; n=30) (Fig. 7C,E). Consistent with the misregulation of *cxcl12b* and *ackr3b* expression observed in *wls* mutants (Fig. 6G-J′), axons that emerge from their smaller dHb are also misdirected (Class II 58.1%, Class III 14%; n=43) (Fig. 7D,E). Thus, although the Cxcr4b-chemokine signaling pathway is not required for the generation of dHb neurons, it is necessary for the correct outgrowth of their efferent axons.

Axon outgrowth from the dHb begins just prior to 2 dpf, with some axon terminals reaching the IPN between 2 and 3 dpf (Beretta et al., 2017; Kuan et al., 2007; Gamse et al., 2005). Cxcr4b receptors are present on the membrane of dHb neurons during this timeframe (Fig. 8A,B), as assayed using the transgenic reporter *TgBAC(cxcr4b:cxcr4b-mKate2-IRES-GFP-CAAX)* (Venkiteswaran et al., 2013). Internalization of the Cxcr4b-mKate2 fusion protein from the GFP-tagged cell membrane is indicative of active chemokine signaling (Venkiteswaran et al., 2013). Cxcr4b-mKate2 labeling is detected in the medioventral region of the dHb, where newly born neurons arise, as well as on their emerging axons. Although GFP labeling of axonal membranes extends from the dHb toward the IPN (Fig. 8A,B, arrows), the mKate2 signal is found on the proximal portion of these efferent projections and is absent more distally (Fig. 8A,B, arrowheads). This distribution of Cxcr4b receptors further supports a role for chemokine signaling in the initial outgrowth of axons from dHb neurons.

DISCUSSION

We investigated the formation of the zebrafish dHb nuclei and examined how the convergence of multiple signaling pathways influences their development and axonal projections. As summarized schematically in Fig. 9, Shh acts upstream or parallel to Wnt signaling, which functions additively with Fgf signaling to generate *dbx1b*-expressing dHb progenitors. The progenitors then give rise to *cxcr4b*-expressing neural precursors that differentiate into the mature neurons of the dHb. A second role for Wnt signaling is to delimit the spatial extent of Fgf activity in the dorsal diencephalon, which, in turn, regulates the expression of *cxcl12b* and *ackr3b* genes in the Cxcr4b chemokine signaling pathway. In the absence of Wnt signaling or upon loss of the Cxcr4b chemokine receptor or Cxcl12a ligand, dHb neurons exhibit aberrant axonal outgrowth.

Identity and differentiation of dHb progenitors

In prior studies, two populations of cells were presumed to correspond to habenular progenitors in zebrafish: cells expressing *cxcr4b* and those expressing *dbx1b* (Roussigné et al., 2009; Halluin et al., 2016; Dean et al., 2014). Because only a small subset of cells shows overlapping expression, we sought to determine the relationship between the cell populations that express these genes.

The earliest known marker of the developing dHb is *dbx1b*, with transcripts detected at 24 hpf (Dean et al., 2014). The *dbx1b*-expressing cells are found in a ventromedial domain relative to mature habenular neurons. Consecutive imaging of the dHb demonstrated that labeling from a *dbx1b* transgenic driver decreases over time, becomes restricted to the most medioventral region, and persists until at least 4 weeks postfertilization. Lineage tracing experiments demonstrate that the *dbx1b*-expressing cells are progenitors, since they give rise to neurons throughout the larval (Dean et al., 2014) as well as the adult dHb. These findings are in agreement with expression analyses of the murine homolog *Dbx1* and lineage studies in the mouse brain (Vue et al., 2007).

Expression of *cxcr4b* in the habenulae is first detected at 28 hpf, 4 h later than *dbx1b* (Roussigné et al., 2009). Time-lapse imaging reveals that *cxcr4b*-expressing cells do not migrate to the developing habenulae from more caudal regions, as was previously proposed (Kuan et al., 2015). Rather, labeling from a *cxcr4b* driver is initiated in a subset of cells that express GFP under the control of a *dbx1b* promoter. This indicates that *cxcr4b*$^{+}$ cells are derived from *dbx1b*$^{+}$ progenitors. Over time, *dbx1b* expression is downregulated in *cxcr4b*$^{+}$ cells, which are found dorsal and lateral to the *dbx1b*$^{+}$ progenitors. Expression of *cxcr4b* is also gradually lost, as cells in more dorsolateral positions begin to express markers of differentiated dHb neurons. The temporal

Development (2017) 144, 2652-2662 doi:10.1242/dev.147751

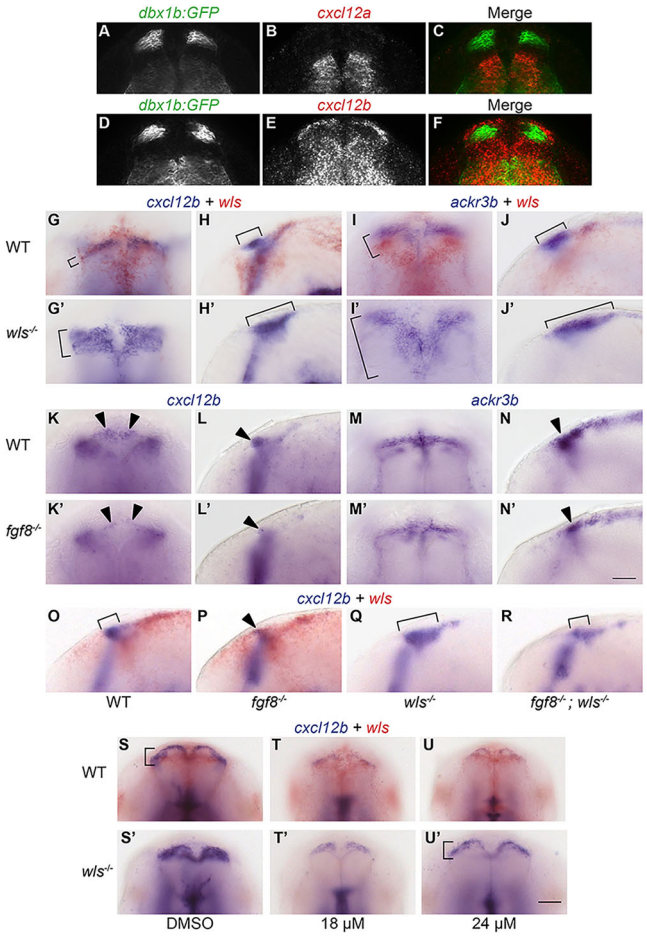

Fig. 6. Fgf signaling regulates expression domains of chemokine pathway components. (A-F) The (A-C) *cxcl12a* and (D-F) *cxcl12b* genes are transcribed in regions adjacent to the dHb at 35 hpf, as shown by fluorescence *in situ* hybridization and immunolabeling for GFP in *TgBAC(dbx1b:GFP)* embryos. (G-H′) *cxcl12b* and (I-J′) *ackr3b* expression domains (brackets) are expanded in *wls* mutants. In *fgf8a* mutants, (K-L′) *cxcl12b* and (M-N′) *ackr3b* dorsal diencephalic expression domains (arrowheads) are reduced. Although the *cxcl12b* expression domain is reduced in (P) *fgf8a* mutants and expanded in (Q) *wls* mutants, (R) *fgf8a;wls* double mutants show a pattern more similar to (O) WT. Between 24 and 48 hpf, WT and *wls* mutant siblings were treated with either (S,S′) 0.3% DMSO, (T,T′) 18 µM SU5402+0.3% DMSO, or (U,U′) 24 µM SU5402+0.3% DMSO. Following treatment with 24 µM SU5402, *cxcl12b* expression in *wls* mutants is restored to the WT pattern (brackets). Scale bar: 30 µm. Refer to Table 1 for numerical values. Dorsal (A-G′,I,I′,K,K′,M, M′,S-U′) and lateral (H,H′,J,J′,L,L′,N,N′,O-R) views are shown. Scale bars: 50 µm.

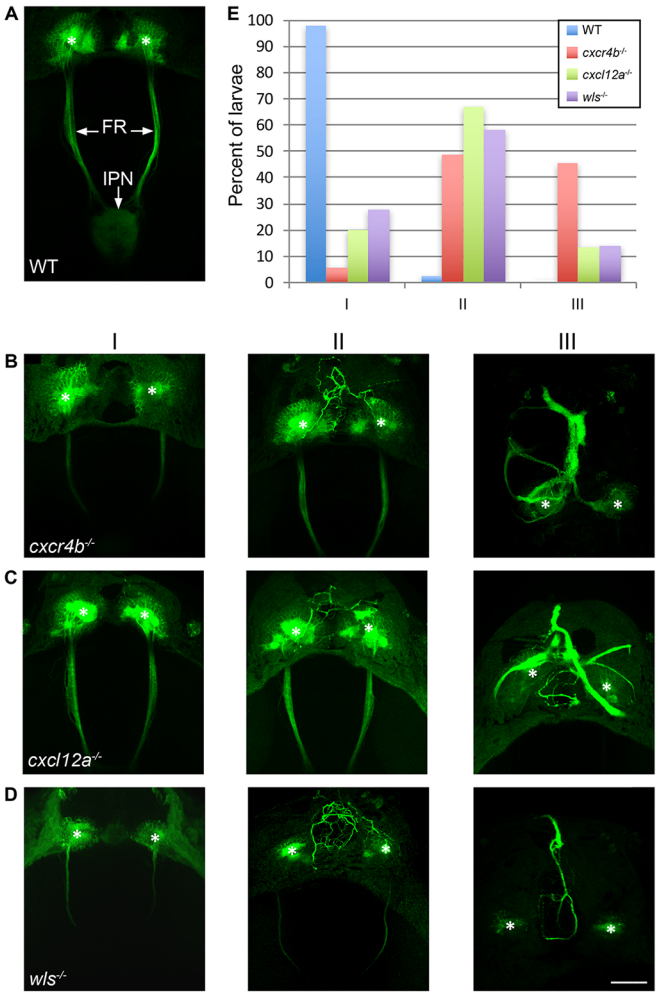

Fig. 7. Chemokine signaling directs outgrowth of dHb axons. (A) In 5 dpf WT larvae, *TgBAC(gng8:CAAX-GFP)* labels neurons in the left and right dHb and their efferent axons in the FR, which terminate at the midbrain IPN. (B-D) Axonal morphology of 5 dpf (B) *cxcr4b*, (C) *cxcl12a* and (D) *wls* mutants falls into three general phenotypic classes: in Class I, the majority of axons fasciculate normally and project posteriorly; in Class II, some ectopic axons extend anterior to the dHb; and in Class III, the majority of axons grow anteriorly and fasciculate as a thick midline bundle. Asterisks indicate the dHb. Scale bar: 50 µm. (E) Percentage of WT siblings (blue, *n*=41) and *cxcr4b* (red, *n*=35), *cxcl12a* (green, *n*=30) and *wls* (purple, *n*=43) mutants with Class I, II or III axonal morphology.

pattern of *cxcr4b* expression parallels the previously described medial to lateral progression of dHb neurogenesis (Aizawa et al., 2007). Persistence of dTomato labeling from *TgBAC(cxcr4b:nls-dTomato)* in mature dHb neurons provides further support that *cxcr4b* expression demarcates a neural precursor population. Thus, development of the dHb is characterized by the transition from *dbx1b*$^{+}$ progenitors to *cxcr4b*$^{+}$ neural precursors and finally to *elavl3*$^{+}$ neurons.

Formation of *dbx1b*$^{+}$ dHb progenitors requires Wnt and Fgf signaling

Disruption of Fgf or Wnt signaling pathways results in small dHb due to a reduction in progenitor cells (Regan et al., 2009; Dean et al., 2014; Kuan et al., 2015). It was previously reported that embryos homozygous for a mutation in *fgf8a* fail to form *dbx1b*$^{+}$ progenitors (Dean et al., 2014). However, we find that *dbx1b*-expressing cells are present in *fgf8a* homozygous mutants at a later stage, although there are considerably fewer than in WT siblings. Fgf signaling could be responsible for generating the appropriate number of progenitors and/or for regulating *dbx1b* transcription. In support of the latter hypothesis, *dbx1b* expression is lost upon treatment of zebrafish embryos with SU5402, an inhibitor of Fgf receptor 1, but restored after its removal (Dean et al., 2014).

Through the analysis of *wls* mutants, we discovered an unsuspected role for the Wnt pathway in spatially restricting expression of *fgf8a*, and thereby limiting the extent of Fgf signaling in the developing dorsal diencephalon. In *wls* mutants, however, increased Fgf signaling does not compensate for the loss of Wnt signaling, as there are still fewer *dbx1b*-expressing dHb progenitors. Furthermore, *wls;fgf8a* double mutants or *wls* mutants treated with SU5402 fail to produce any *dbx1b*$^{+}$ progenitors, indicating that the two signaling pathways work in an additive manner to generate the dHb progenitor population.

Development (2017) 144, 2652-2662 doi:10.1242/dev.147751

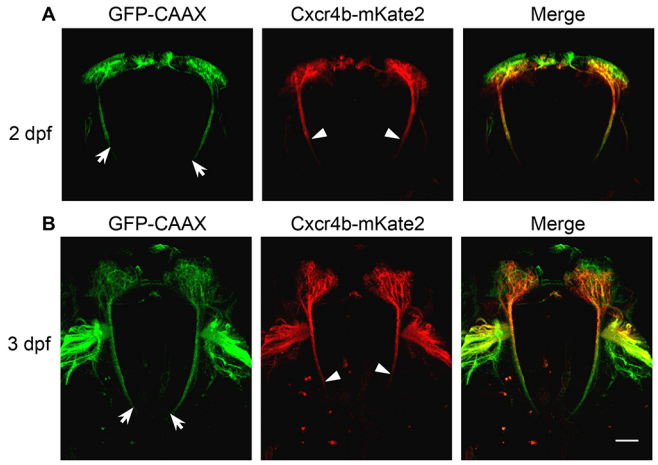

Fig. 8. Chemokine signaling reporter labels newly born neurons and emerging axons. *TgBAC(cxcr4b:cxcr4b-mKate2-IRES-GFP-CAAX)* labeling at (A) 2 and (B) 3 dpf. GFP labels the membranes of dHb neurons and axons. The Cxcr4b chemokine receptor fusion protein (red) is found in neurons near the ventricular zone and on proximal (arrowheads) but not distal (arrows) regions of their axons. Scale bar: 50 µm.

One hypothesis is that Wnt establishes a 'pro-habenular' territory, in which cells express *dbx1b* only after activation by Fgf signaling. Loss of Wnt signaling, as in *wls* mutants, results in smaller pro-habenulae and, therefore, fewer cells that could express *dbx1b*, irrespective of the level of Fgf signaling. This is a challenging hypothesis to test because *dbx1b* expression is the earliest known indicator of dHb formation.

Recent studies have also implicated Hh signaling as an early regulator of habenular development (Chatterjee et al., 2014; Halluin et al., 2016). In zebrafish embryos homozygous for a mutation in the *smo* gene, which encodes a G protein-coupled receptor essential for Hh signaling, expression of *cxcr4b* was reported as absent in the epithalamic region in one study (Halluin et al., 2016) and expanded in another (Chatterjee et al., 2014). In our experiments, neither *cxcr4b* nor *dbx1b* transcripts were detected in this region of the *smo* mutant brain. Thus, Hh signaling is required to produce dHb progenitors and/or to induce *dbx1b* expression. Based on these results, and the finding that expression of *shha* is unperturbed in the ZLI of *wls* homozygotes, we presume that the Hh pathway acts upstream of or parallel to Wnt signaling in defining the pro-habenular territory.

Fgf and Wnt signaling regulate expression of chemokine pathway components

Homozygous *fgf8a* mutants show reduced expression of genes encoding the chemokine signaling components Cxcl12b and Ackr3b. However, in *wls* mutants, *fgf8a* expression and Fgf signaling domains are dramatically enlarged, and, as a consequence, so are the *cxcl12b* and *ackr3b* expression domains. Reduction of Fgf signaling in *wls* mutants by mutation of *fgf8a* or chemical inhibition restores *cxcl12b* expression to a WT pattern. These results demonstrate that Fgf8a normally functions downstream of Wnt signaling to define the spatial expression of chemokine pathway components in regions surrounding the habenulae.

A regulatory relationship between Wnt signaling, Fgf signaling and *ackr3b* expression was previously reported in the migrating lateral line primordia of zebrafish (Aman and Piotrowski, 2008). In this tissue, Fgf induces the expression of Wnt inhibitors, whereas Wnt induces expression of both Fgf ligands and Fgf signaling inhibitors (Aman and Piotrowski, 2008). This creates mutually exclusive regions of Wnt and Fgf signaling, where Wnt signaling is active at the leading tip of the migratory primordium and Fgf signaling occurs in the trailing zone. Expression of *ackr3b* is spatially restricted to the trailing cells, but it is unclear whether this is caused by inhibition by Wnt in the leading zone, or by activation by Fgf and/or relief of Wnt inhibition in the trailing cells. Although the precise genetic interactions in the lateral line may differ from those in the dorsal diencephalon, there are parallels between the two, as both tissues rely on the opposing forces of Wnt and Fgf signaling to regulate the spatial expression pattern of a chemokine receptor.

The Cxcr4-chemokine pathway directs habenular axon outgrowth

We have uncovered a new role for the Cxcr4-chemokine pathway in the establishment of dHb-IPN connectivity. Although *cxcr4b* transcription is downregulated in dHb neurons, the protein likely persists, as evidenced by labeling of a Cxcr4b fluorescent fusion protein. Loss of the chemokine receptor results in atypical rostral projections of habenular efferents. Similar axonal phenotypes are observed in mutants lacking the Cxcl12a chemokine ligand and in *wls* mutants, in which expression of genes encoding the Cxcl12b chemokine and the chemokine receptor Ackr3b are both misregulated.

The function of Cxcl12 chemokines in axonal pathfinding is complex and depends on the neuronal type being assayed. For example, Cxcl12 is a repulsive cue for efferents of rat cerebellar neurons (Xiang et al., 2002), but an attractant for axons of retinal ganglion cells (Li et al., 2005), and creates a permissive environment for a number of cell types including olfactory neurons (Miyasaka et al., 2007), retinal ganglion cells (Chalasani et al., 2003a, 2007), dorsal root ganglia neurons (Chalasani et al., 2003b) and ventral motor neurons (Lieberam et al., 2005).

The projection defects of dHb neurons that result from loss of Cxcr4b could, thus, be caused by the inability of their axons to respond to a posterior attractive cue and/or an anterior repulsive cue. The *cxcl12a* gene is expressed posterior to the developing habenulae. The defects in axonal outgrowth observed in *cxcl12a* mutants indicate that the chemokine might serve as an attractant that guides axons caudally, or, alternatively, creates a permissive environment for dHb axon outgrowth. Conversely, *cxcl12b* transcripts are abundant anterior to the dHb, suggesting that Cxcl12b repels axons from extending rostrally. An examination of *cxcl12b* mutants is required to test this hypothesis. The defective axonal outgrowth phenotype is less penetrant in *cxcl12a* mutants than in *cxcr4b* mutants, suggesting that the Cxcl12a and Cxcl12b ligands might act in conjunction to regulate the direction of dHb axonal outgrowth.

In *wls* mutants, expression of *cxcl12a* is unaltered and *cxcr4b* is expressed in the developing dHb, yet axons still project aberrantly. The gene encoding the Cxcl12b ligand is inappropriately transcribed throughout the dHb. High levels of chemokines have been reported to function as dominant negatives for chemokine signaling by binding to and driving internalization of the receptor (Miyasaka et al., 2007). It is possible that the expanded *cxcl12b* expression in *wls* mutants also has a dominant-negative effect, resulting in aberrant, anteriorly directed axonal outgrowth. In *cxcr4b*, *cxcl12a* and *wls* mutants, the many rostrally directed axons from both the left and right dHb extend toward the midline, where they fasciculate and project anteriorly as a single bundle (Class III phenotype). This suggests that, in the absence of normal chemokine signaling, these axons can now respond inappropriately to an anterior midline cue.

Development (2017) 144, 2652-2662 doi:10.1242/dev.147751

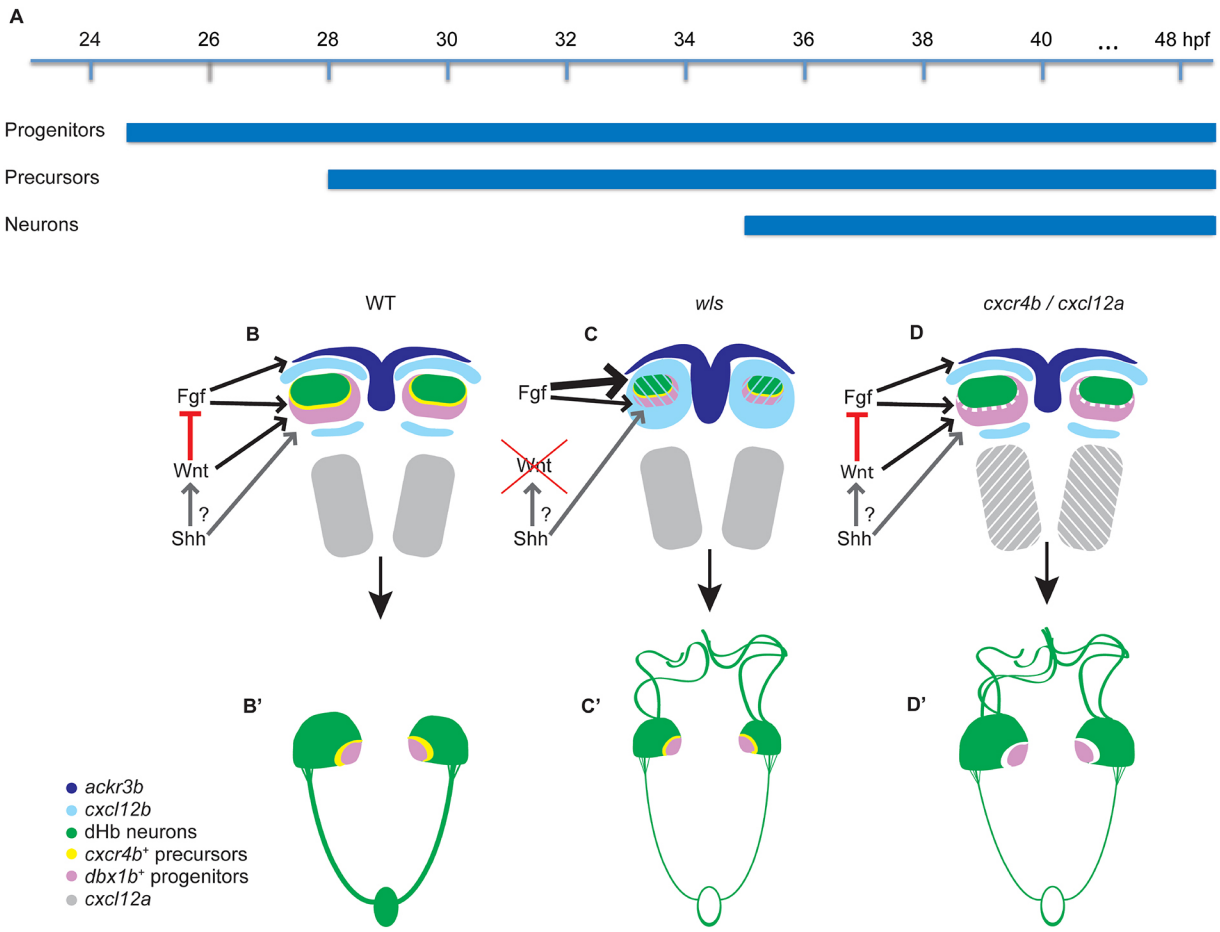

Fig. 9. Schematic of signaling pathways in dHb development. (A) Timeline indicating when *dbx1b*$^{+}$ progenitors, *cxcr4b*$^{+}$ precursors and *ano2*$^{+}$ neurons are detected in the developing dHb. (B) In zebrafish embryos, Wnt and Fgf signaling function additively to generate *dbx1b*$^{+}$ progenitors (purple), which produce *cxcr4b*$^{+}$ neural precursors (yellow) that differentiate into habenular neurons (green). Shh acts upstream of or parallel to Wnt and Fgf signaling. The Wnt pathway also regulates the spatial extent of Fgf signaling, which in turn confines *cxcl12b* (light blue) and *ackr3b* (dark blue) transcription to regions anterior of the developing dHb. *cxcl12a* (gray) transcripts are present in bilateral domains posterior and ventral to the habenular region. Establishing this spatial pattern of chemokine signaling later influences the outgrowth of dHb efferents. (B′) In WT larvae, anterior inhibition or posterior attraction directs outgrowth of dHb axons caudally towards the IPN. (C) In *wls* mutants, Wnt signaling is disrupted, *dbx1b*$^{+}$ progenitors are reduced, and the dHb are significantly smaller (Kuan et al., 2015). Additionally, Fgf signaling is expanded, as are *cxcl12b* and *ackr3b* domains of expression, resulting in ectopic chemokine signaling and (C′) aberrant rostral projections from dHb neurons. (D) In mutants lacking either the Cxcr4b chemokine receptor (dashed line) or the Cxcl12a chemokine (hatched area) formation of the dHb appears normal, but (D′) dHb axon outgrowth is aberrant.

These results indicate that chemokine signaling influences the direction of dHb axon outgrowth, and is reminiscent of the action of ventral motor neuron axons, which upon loss of chemokine signaling choose the exit point of dorsal motor neurons (Lieberam et al., 2005). Axons that do emerge caudally from mutant dHb successfully join the FR and innervate the IPN. Successful pathfinding by this subset of axons indicates that other signaling pathways mediate axon fasciculation, extension of the FR through the midbrain, and target recognition. Several axon guidance cues and receptors have been implicated in aspects of this process including Netrin/DCC (Schmidt et al., 2014; Funato et al., 2000), Sema3F/Nrp2 (Giger et al., 2000; Chen et al., 2000; Sahay et al., 2003), Sema5A (Kantor et al., 2004) and Sema3D/Nrp1a (Kuan et al., 2007). Disruption of most components leads to defasciculation of the FR or to incorrect innervation of the IPN. Only the loss of DCC or Netrin results in ectopic projections outside the FR (Schmidt et al., 2014).

If the chemokine signaling pathway is not required for guidance of dHb neurons to the target, but rather influences the initial outgrowth of their axons, newly born dHb neurons and their emerging axons, but not older neurons or axons approaching or innervating the IPN, would be expected to respond to chemokine signals. Indeed, labeling by the Cxcr4b fluorescent fusion protein is detected in medially positioned neurons found closest to the ventricular zone. Receptors are also enriched in axons newly emerging from the dHb, but are absent distally as they extend closer to the IPN. This distribution of Cxcr4b receptors suggests that they are rapidly internalized upon chemokine binding and degraded as axons elongate.

Understanding the processes underlying development of the habenular nuclei and the generation of their neuronal diversity and connectivity is key to unraveling their roles in behavior and mood disorders. Integration of the multiple genes and signaling pathways implicated in dHb development is an important step toward determining how their neurons arise and form appropriate synaptic connections.

MATERIALS AND METHODS

Zebrafish husbandry

Zebrafish were kept on a 14 h-light/10 h-dark cycle at 27°C. Embryos were raised in system water or, for experiments, maintained in system water with 0.003% phenylthiourea (1× PTU) to reduce pigmentation. The AB WT

Development (2017) 144, 2652-2662 doi:10.1242/dev.147751

strain (Walker, 1998) and lines bearing the *wls*^{c186} (Kuan et al., 2015), *fgf8*^{ti282a} (Brand et al., 1996), *cxcr4b*^{t26035} (Knaut et al., 2003) and *smo*^{hi1640Tg} (Chen et al., 2001) mutations were used. Homozygous *wls*^{c186} mutants were genotyped as embryos or identified as larvae according to morphological criteria (Kuan et al., 2015). Embryos and larvae homozygous for *cxcr4b*^{t26035} were genotyped using published primers (Miyasaka et al., 2007). The transgenic lines used include *TgBAC(gng8:Eco.NfsB-2A-CAAX-GFP)* [referred to as *Tg(gng8:CAAX-GFP)*] (deCarvalho et al., 2013), *TgBAC(dbx1b:Cre-mCherry)* (Koyama et al., 2011), *TgBAC(cxcr4b:nls-dTomato)* (Donà et al., 2013), *TgBAC(dbx1b:GFP)* (Kinkhabwala et al., 2011), *Tg(hsp70:dkk1-GFP)* (Stoick-Cooper et al., 2007), *TgBAC(dbx1b:tdTomato-nls)* (Satou et al., 2012), *Tg(HuC:H2B-GCamP6S)* (Vladimirov et al., 2014), *TgBAC(cxcr4b:cxcr4b-mKate2-IRES-GFP-CAAX)* (Venkiteswaran et al., 2013) and *Tg(β-actin:loxP-hmgb1-eCFP-loxP-H2B-mCherry)* (M. Parsons, Johns Hopkins University, Baltimore, MD, USA, unpublished). Zebrafish maintenance and experimental procedures were performed according to protocols approved by the Carnegie Institution for Science Animal Care and Use Committee.

RNA *in situ* hybridization and immunofluorescence

Colorimetric and fluorescent *in situ* hybridization were performed according to previously described methods (deCarvalho et al., 2013). RNA probes were synthesized for *dbx1b* (Gribble et al., 2007), *etv5b*, *ackr3b*, *cxcr4b*, *wls* (Thisse et al., 2001), *fgf8* (Fürthauer et al., 1997), *ano2* (deCarvalho et al., 2014), *dusp6* (Tsang et al., 2004), *cxcl12a* (Doitsidou et al., 2002), *cxcl12b* (Thisse and Thisse, 2005) and *elavl3* (Kim et al., 1996). GFP was detected using rabbit antisera (TP401, Torrey Pines Biolabs) and a Cy3-conjugated AffiniPure anti-rabbit IgG secondary antibody (1:500, 111-165-144, Jackson ImmunoResearch). Immunolabeling was performed as described (deCarvalho et al., 2013).

Inhibition of signaling pathways

To inhibit Wnt signaling, *Tg(hsp70:dkk1-GFP)* embryos were heat shocked at 24 hpf according to published methods (Stoick-Cooper et al., 2007). For inhibition of Fgf signaling, embryos were maintained in 1× PTU and, between 24 and 48 hpf, treated with the FGFR inhibitor SU5402 (12-24 µM, SML0043, Sigma-Aldrich) in 0.3% dimethyl sulfoxide (DMSO) or exposed to vehicle alone. Embryos were washed for 5 min before fixation in 4% paraformaldehyde (PFA).

Sectioning and microscopy

A Zeiss AxioCam HRc camera mounted on a Zeiss Axioskop was used to obtain bright-field images. Fluorescent images were captured on an upright or inverted Leica SP5 confocal microscope fitted with a 25×/0.95 NA water immersion objective. Fixed and live embryos were mounted in 1.2% low-melt agarose (SeaPlaque, Lonza) in 1× phosphate buffered saline (PBS) or fish system water with 200 mg/l tricaine (Sigma-Aldrich), respectively. Sectioning and imaging of adult brains was performed as previously described (deCarvalho et al., 2014), and sections were cut every 60 µm.

Image analysis and statistics

Confocal images were analyzed using Imaris software (Bitplane). Measurements obtained from colormetric *in situ* hybridization images were collected using the Fiji imaging processing package (https://fiji.sc/) (Schindelin et al., 2012; Schindelin et al., 2015) and provided as the mean ±s.e.m. Statistical analyses were performed using the Student's two-tailed *t*-test (Microsoft Excel).

Time-lapse imaging

Embryos were sedated in 165 mg/l tricaine in 1× PTU and mounted in 1% low-melt agarose in a glass-bottomed dish (WillCo Wells). These tricaine and agarose concentrations were shown to reduce developmental defects in long-term imaging experiments (Kaufmann et al., 2012). Time-lapse imaging was performed on a Leica SP5 inverted confocal microscope with a 25×/NA 0.95 water immersion lens. *Z*-stacks of the dorsal embryonic brain (~100-300 µm, step size 1 µm) were acquired at 15 min intervals. Imaging was performed for 24 h, during which deionized water was continually pumped between the objective and glass-bottomed dish. A metal collar (Leica Water Immersion Micro Dispenser cap) was mounted over the objective and attached to a 10 ml syringe using flexible polymer tubing (Tygon). The syringe was placed in a syringe pump (NE-300, New Era Pump Systems), which was set to dispense at a rate of 40 µl/h.

Acknowledgements

We thank Stephen Devoto, Richard Dorsky, Joshua Gamse, Darren Gilmour, Holger Knaut, Michael Parsons and Michael Tsang for providing reagents and mutant and transgenic zebrafish; Holger Knaut for his valuable advice on experimental design; Michelle Macurak for technical assistance; and Andrew Rock and Carmen Tull for care of the aquatics facility.

Competing interests

The authors declare no competing or financial interests.

Author contributions

Conceptualization: S.R., M.E.H.; Methodology: S.R.; Investigation: S.R.; Data curation: S.R.; Writing - original draft: S.R.; Writing - review & editing: S.R., M.E.H.; Supervision: M.E.H.; Project administration: M.E.H.; Funding acquisition: M.E.H.

Funding

This study was supported by the Eunice Kennedy Shriver National Institute of Child Health and Human Development (R01HD042215 to M.E.H.). Deposited in PMC for release after 12 months.

Supplementary information

Supplementary information available online at
http://dev.biologists.org/lookup/doi/10.1242/dev.147751.supplemental

References

Aizawa, H., Goto, M., Sato, T. and Okamoto, H. (2007). Temporally regulated asymmetric neurogenesis causes left-right differences in the zebrafish habenular structures. *Dev. Cell* **12**, 87-98.

Aizawa, H., Amo, R. and Okamoto, H. (2011). Phylogeny and ontogeny of the habenular structure. *Front. Neurosci.* **5**, 138.

Aman, A. and Piotrowski, T. (2008). Wnt/β-catenin and Fgf signaling control collective cell migration by restricting chemokine receptor expression. *Dev. Cell* **15**, 749-761.

Antolin-Fontes, B., Ables, J. L., Görlich, A. and Ibañez-Tallon, I. (2015). The habenulo-interpeduncular pathway in nicotine aversion and withdrawal. *Neuropharmacology* **96**, 213-222.

Baldwin, P. R., Alanis, R. and Salas, R. (2011). The role of the habenula in nicotine addiction. *J. Addict. Res. Ther.* **S1**, 002.

Benarroch, E. E. (2015). Habenula: recently recognized functions and potential clinical relevance. *Neurology* **85**, 992-1000.

Beretta, C. A., Dross, N., Guglielmi, L., Bankhead, P., Soulika, M., Gutierrez-Triana, J. A., Paolini, A., Poggi, A., Falk, J., Ryu, S. et al. (2017). Early commissural diencephalic neurons control habenular axon extension and targeting. *Curr. Biol.* **27**, 270-278.

Boldajipour, B., Mahabaleshwar, H., Kardash, E., Reichman-Fried, M., Blaser, H., Minina, S., Wilson, D., Xu, Q. and Raz, E. (2008). Control of chemokine-guided cell migration by ligand sequestration. *Cell* **132**, 463-473.

Braitenberg, V. and Kemali, M. (1970). Exceptions to bilateral symmetry in the epithalamus of lower vertebrates. *J. Comp. Neurol.* **138**, 137-146.

Brand, M., Heisenberg, C. P., Jiang, Y. J., Beuchle, D., Lun, K., Furutanit-Seiki, M., Granato, M., Haffter, P., Hammerschmidt, M., Kane, D. A. et al. (1996). Mutations in zebrafish genes affecting the ormation of the boundary between midbrain and hindbrain. *Development* **123**, 179-190.

Chalasani, S., Baribaud, F., Coughlan, C. M., Sunshine, M. J., Lee, V. M., Doms, R. W., Littman, D. R. and Raper, J. A. (2003a). The chemokine stromal cell-derived factor-1 promotes the survival of embryonic retinal ganglion cells. *J. Neurosci.* **23**, 4601-4612.

Chalasani, S., Sabelko, K. A., Sunshine, M. J., Littman, D. R. and Raper, J. A. (2003b). A chemokine Sdf-1 reduces the effectiveness of multiple axonal repellants and is required for normal axon pathfinding. *J. Neurosci.* **23**, 1360-1371.

Chalasani, S., Sabol, A., Xu, H., Gyda, M. A., Rasband, K., Granato, M., Chien, C. B. and Raper, J. A. (2007). Stromal cell-derived factor-1 antagonizes slit/robo signaling *in vivo*. *J. Neurosci.* **27**, 973-980.

Chatterjee, M., Guo, Q., Weber, S., Schlopp, S. and Li, J.Y. (2014). Pax6 regulates the formation of the habenular nuclei by controlling the temporospatial expression of Shh in the diencephalon in vertebrates. *BMC Biol.* **12**, 13.

Development (2017) 144, 2652-2662 doi:10.1242/dev.147751

Chen, H., Bagri, A., Zupicich, J. A., Zou, Y., Stoeckli, E., Pleasure, S. J., Lowenstein, D. H., Skarnes, W. C., Chédotal, A. and Tessier-Lavigne, M. (2000). Neuropilin-2 regulates the development of selective cranial and sensory nerves and hippocampal mossy fiber projections. *Neuron* **25**, 43-56.

Chen, W., Burgess, S. and Hopkins, N. (2001). Analysis of the zebrafish smoothened mutant reveals conserved and divergent functions of the hedgehog activity. *Development* **128**, 2385-2396.

Concha, M. L. and Wilson, S. W. (2001). Asymmetry in the epithalamus of vertebrates. *J. Anat.* **199**, 63-84.

Dambly-Chaudiere, C., Cubedo, N. and Ghysen, A. (2007). Control of cell migration in the development of the posterior lateral line: antagonistic interactions between the chemokine receptors CXCR4 and CXCR7/RDC1. *BMC Dev. Biol.* **7**, 23.

Dean, B. J., Erdogan, B., Gamse, J. T. and Wu, S.-Y. (2014). Dbx1b defines the dorsal habenular progenitor domain in the zebrafish epithalamus. *Neural Dev.* **9**, 20.

deCarvalho, T. N., Akitake, C. M., Thisse, C., Thisse, B. and Halpern, M. E. (2013). Aversive cues fail to activate fos expression in the asymmetric olfactory-habenula pathway of zebrafish. *Front. Neural Circuits* **7**, 98.

deCarvalho, T. N., Subedi, A., Rock, J., Harfe, B. D., Thisse, C., Thisse, B., Halpern, M. E. and Hong, E. (2014). Neurotransmitter map of the asymmetric dorsal habenular nuclei of zebrafish. *Genesis* **52**, 636-655.

Doitsidou, M., Reichman-Fried, M., Stebler, J., Köprunner, M., Dörries, J., Meyer, D., Esguerra, C. V., Leung, T. and Raz, E. (2002). Guidance of primordial germ cell migration by the chemokine SDF-1. *Cell* **111**, 647-659.

Donà, E., Barry, J. D., Valentin, G., Quirin, C., Khmelinskii, A., Kunze, A., Durdu, S., Newton, L. R., Fernandez-Minan, A., Huber, W. et al. (2013). Directional tissue migration through a self-generated chemokine gradient. *Nature* **503**, 285-289.

Duboué, E. and Halpern, M. E. (2017). Genetic and transgenic approaches to study zebrafish brain asymmetry and lateralized behavior. In *Lateralized Brain Function: Methods in Human and Non-Human Species* (ed. L. J. Rogers and G. Vallortigara), Neuromethods 122, pp. 553-589. New York: Humana Press.

Fowler, C. D., Lu, Q., Johnson, P. M., Marks, M. J. and Kenny, P. J. (2011). Habenular a5 nicotinic receptor signaling controls nicotine intake. *Nature* **471**, 597-601.

Funato, H., Saito-Nakazato, Y. and Takahashi, H. (2000). Axonal growth from the habenular nucleus along the neuromere boundary region of the diencephalon is regulated by semaphorin 3F and netrin-1. *Mol. Cell. Neurosci.* **16**, 206-220.

Fürthauer, M., Thisse, C. and Thisse, B. (1997). A role for FGF-8 in the dorsoventral patterning of the zebrafish gastrula. *Development* **124**, 4253-4264.

Gamse, J. T., Kuan, Y.-S., Macurak, M., Brösamle, C., Thisse, B., Thisse, C. and Halpern, M. E. (2005). Directional asymmetry of the zebrafish epithalamus guides dorsoventral innervation of the midbrain target. *Development* **132**, 4869-4881.

Giger, R. J., Cloutier, J.-F., Sahay, A., Prinjha, R. K., Levengood, D. V., Moore, S. E., Pickering, S., Simmons, D., Rastan, S., Walsh, F. S. et al. (2000). Neuropilin-2 is required *in vivo* for selective axon guidance responses to secreted semaphorins. *Neuron* **25**, 29-41.

Gribble, S. L., Nikolaus, O. B. and Dorsky, R. I. (2007). Regulation and function of *dbx* genes in the zebrafish spinal cord. *Dev. Dyn.* **236**, 3472-3483.

Güntürkün, O. and Ocklenburg, S. (2017). Ontogenesis of lateralization. *Neuron* **94**, 249-263.

Halluin, C., Madelaine, R., Naye, F., Peers, B., Roussigné, M. and Blader, P. (2016). Habenular neurogenesis in zebrafish is regulated by a hedgehog, Pax6 proneural gene cascade. *PLoS ONE* **11**, e0158210.

Kantor, D., Chivatakarn, O., Peer, K. L., Oster, S. F., Inatani, M., Hansen, M. J., Flanagan, J. G., Yamaguchi, Y., Sretavan, D. W., Giger, R. J. et al. (2004). Semaphorin5A is a bifunctional axon guidance cue regulated by heparan and chondroitin sulfate proteoglycans. *Neuron* **44**, 961-975.

Kaufmann, A., Mickoleit, M., Weber, M. and Huisken, J. (2012). Multilayer mounting enables long-term imaging of zebrafish development in a light sheet microscope. *Development* **139**, 3242-3247.

Kim, C.-H., Ueshima, E., Muraoka, O., Tanaka, H., Yeo, S.-Y., Huh, T.-L. and Miki, N. (1996). Zebrafish *elavl/HuC* homologue as a very early neuronal marker. *Neurosci. Lett.* **216**, 109-112.

Kinkhabwala, A., Riley, M., Koyama, M., Monen, J., Satou, C., Kimura, Y., Higashijima, S.-i. and Fetcho, J. (2011). A structural and functional ground plan for neurons in the hindbrain of zebrafish. *Proc. Natl. Acad. Sci. USA* **108**, 1164-1169.

Knaut, H., Werz, C., Geisler, R., Nüsslein-Volhard, C.; The Tübingen 2000 Screen Consortium. (2003). A zebrafish homologue of the chemokine receptor Cxcr4 is a germ-cell guidance receptor. *Nature* **421**, 279-282.

Koyama, M., Kinkhabwala, A., Satou, C., Higashijima, S.-i. and Fetcho, J. (2011). Mapping a sensory-motor network onto a structural and functional ground plan in the hindbrain. *Proc. Natl. Acad. Sci. USA* **108**, 1170-1175.

Kuan, Y.-S., Gamse, J. T., Schreiber, A. M. and Halpern, M. E. (2007). Selective asymmetry in a conserved forebrain to midbrain projection. *J. Exp. Zool.* **308**, 669-678.

Kuan, Y.-S., Roberson, S., Akitake, C. M., Fortuno, L., Gamse, J., Moens, C. and Halpern, M. E. (2015). Distinct requirements for Wntless in habenular development. *Dev. Biol.* **406**, 117-128.

Lawson, R. P., Nord, C. L., Seymour, B. Thomas, D. L., Dayan, P., Pilling, S. and Roiser, J. P. (2016). Disrupted habenula function in major depression. *Mol. Psychiatr.* **22**, 202-208.

Lewellis, S. W. and Knaut, H. (2012). Attractive guidance: how the chemokine SDF1/CXCL12 guides different cells to different locations. *Semin. Cell Dev. Biol.* **23**, 333-340.

Li, Q., Shiarbe, K., Thisse, C., Thisse, B., Okamoto, H., Masai, I. and Kuwada, J. Y. (2005). Chemokine signaling guides axons within the retina in zebrafish. *J. Neurosci.* **25**, 1711-1717.

Lieberam, I., Agalliu, D., Nagasawa, T., Ericson, J. and Jessell, T. M. (2005). A Cxcl12-Cxcr4 chemokine signaling pathway defines the initial trajectory of mammalian motor neurons. *Neuron* **47**, 667-679.

Miyasaka, N., Knaut, H. and Yoshihara, Y. (2007). Cxcl2/Cxcr4 chemokine signaling is required for placode assembly and sensory axon pathfinding in the zebrafish olfactory system. *Development* **134**, 2459-2468.

Namboodiri, V. M. K., Rodriguez-Romaguera, J. and Stuber, G. D. (2016). The habenula. *Curr. Biol.* **26**, R873-R877.

Palevitch, O., Abraham, E., Borodovsky, N., Levkowitz, G., Zohar, Y. and Gothilf, Y. (2010). Cxcl12a-Cxcr4b signaling is important for proper development of the forebrain GnRH system in zebrafish. *Gen. Comp. Endocrinol.* **165**, 262-268.

Pang, X., Liu, L., Ngolab, J., Zhao-Shea, R., McIntosh, J. M., Gardner, P. D. and Tapper, A. R. (2016). Habenular cholinergic neurons regulate anxiety during nicotine withdrawal via nicotinic acetylcholine receptors. *Neuropharmacology* **107**, 294-304.

Ranft, K., Dobrowolny, H., Krell, D., Bielau, H., Bogerts, B. and Bernstein, H. G. (2010). Evidence for structural abnormalities of the human habenular complex in affective disorders but not in schizophrenia. *Psychol. Med.* **40**, 557-567.

Regan, J. C., Concha, M. L., Roussigne, M., Russell, C. and Wilson, S. W. (2009). An Fgf8-bistable cell migratory event establishes CNS asymmetry. *Neuron* **61**, 27-34.

Roussigné, M., Bianco, I. H., Wilson, S. W. and Blader, P. (2009). Nodal signalling imposes left-right asymmetry upon neurogenesis in the habenular nuclei. *Development* **136**, 1549-1557.

Sahay, A., Molliver, M. E., Ginty, D. D. and Kolodkin, A. L. (2003). Semaphorin3F is critical for development of limbic system circuitry and is required in neurons for selective CNS axon guidance events. *J. Neurosci.* **23**, 6671-6680.

Salas, R., Sturm, R., Boulter, J. and De Biasi, M. (2009). Nicotinic receptors in the habenulo-interpeduncular system are necessary for nicotine withdrawal in mice. *J. Neurosci.* **29**, 3014-3018.

Satou, C., Kimura, Y. and Higashijima, S.-i. (2012). Generation of multiple classes of V0 neurons in zebrafish spinal cord: progenitor heterogeneity and temporal control of neuronal diversity. *J. Neurosci.* **32**, 1771-1783.

Savitz, J. B., Nugent, A. C., Bogers, W., Roiser, J. P., Bain, E. E., Neumeister, A., Zarate, C. A., Manji, H. K., Cannon, D. M., Marrett, S. et al. (2011). Habenula volume in bipolar disorder and major depressive disorder: a high-resolution magnetic resonance imaging study. *Biol. Psychiatry* **69**, 336-343.

Schindelin, J., Arganda-Carreras, I., Frise, E., Kaynig, V., Longair, M., Pietzsch, T., Preibisch, S., Rueden, C., Saalfeld, S., Schmid, B. et al. (2012). Fiji: an open-source platform for biological-image analysis. *Nat. Methods* **9**, 676-682.

Schindelin, J., Rueden, C. T., Hiner, M. C. and Eliceiri, K. W. (2015). The ImageJ ecosystem: an open platform for biomedical image analysis. *Mol. Reprod. Dev.* **82**, 518-529.

Schmidt, E. R. E., Brignani, S., Adolfs, Y., Lemstra, S., Demmers, J., Vidaki, M., Donahoo, A.-L. S., Lillevali, K., Vasar, E., Richards, L. J. et al. (2014). Subdomain-mediated axon-axon signaling and chemoattraction cooperate to regulate afferent innervation of the lateral habenula. *Neuron* **82**, 372-387.

Stoick-Cooper, C. L., Weidinger, G., Riehle, K. J., Hubbert, C., Major, M. B., Fausto, N. and Moon, R. T. (2007). Distinct Wnt signaling pathways have opposing roles in appendage regeneration. *Development* **134**, 479-489.

Sutherland, R. J. (1982). The dorsal diencephalic conduction system: a review of the anatomy and functions of the habenular complex. *Neurosci. Biobehav. Rev.* **6**, 1-13.

Thisse, B. and Thisse, C. (2005). High throughput expression analysis of ZF-models consortium clones. *ZFIN Direct Data Submission* (https://zfin.org/ZDB-PUB-051025-1).

Thisse, B., Pfumio, S., Fürthauer, M., Loppin, B., Heyer, V., Degrave, A., Woehl, R., Lux, A., Steffan, T., Charbonnier, X. Q. and Thisse, C. (2001). Expression of the zebrafish genome during embryogenesis. *ZFIN Direct Data Submission* (https://zfin.org/ZDB-PUB-010810-1).

Tsang, M., Maegawa, S., Kiang, A., Habas, R., Weinberg, E. and Dawid, I. B. (2004). A role for MKP3 in axial patterning of the zebrafish embryo. *Development* **131**, 2769-2779.

Venkiteswaran, G., Lewellis, S. W., Wang, J., Reynolds, E., Nicholson, C. and Knaut, H. (2013). Generation and dyanmics of an endogenous, self-generated signaling gradient across a migrating tissue. *Cell* **155**, 674-687.

Development (2017) 144, 2652-2662 doi:10.1242/dev.147751

Vladimirov, N., Mu, Y., Kawashima, T., Bennett, D. V., Yang, C. T., Looger, L. L., Keller, P. J., Freeman, J. and Ahrens, M. B. (2014). Light-sheet functional imaging in fictively behaving zebrafish. *Nat. Methods* **11**, 883-884.

Vue, T. Y., Aaker, J., Taniguchi, A., Kazemzadeh, C., Skidmore, J. M., Martin, D. M., Martin, J. F., Treier, M. and Nakagawa, Y. (2007). Characterization of progenitor domains in the developing mouse thalamus. *J. Comp. Neurol.* **505**, 73-91.

Walker, C. (1998). Haploid screens and gamma-ray mutagenesis. *Methods Cell Biol.* **60**, 43-70.

Xiang, Y., Li, Y., Zhang, Z., Cui, K., Wang, S., Yuan, X. B., Wu, C. P., Poo, M. M. and Duan, S. (2002). Nerve growth cone guidance mediated by G protein-coupled receptors. *Nat. Neurosci.* **5**, 843-848.

Zhao-Shea, R., Liu, L., Pang, X., Gardner, P. D. and Tapper, A. R. (2013). Activation of GABAergic neurons in the interpeduncular nucleus triggers physical nicotine withdrawal symptoms. *Curr. Biol.* **23**, 2327-2335.

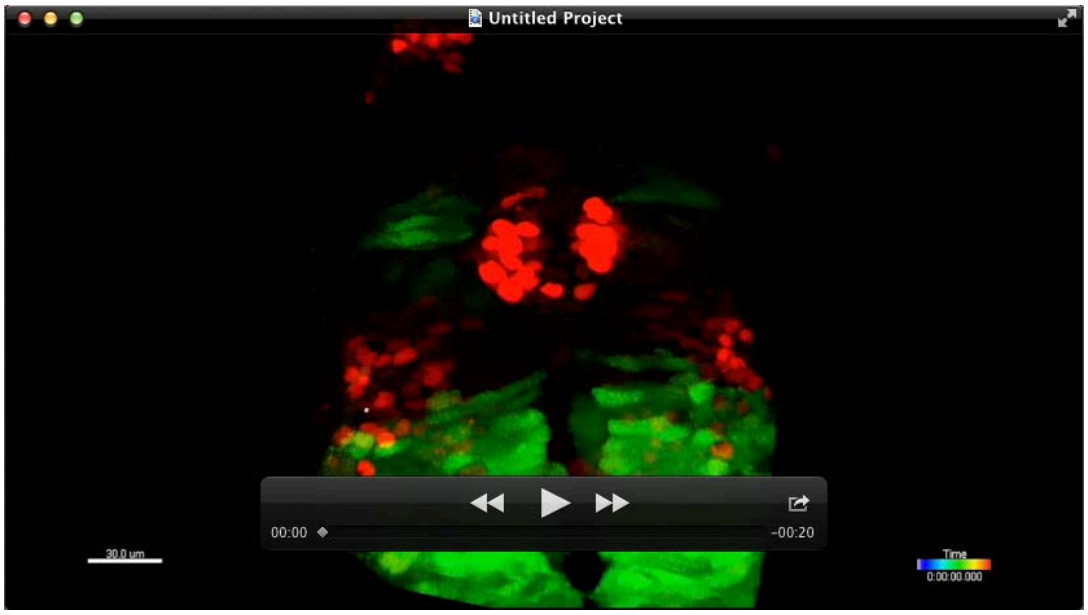

Movie 1: Time lapse imaging of *dbx1b*$^{+}$ and *cxcr4b*$^{+}$ labeled populations.

Time lapse imaging of a doubly labeled *TgBAC(dbx1b:GFP)* and *TgBAC(cxcr4b:nls-tdTomato)* embryo between 27 and 48 hpf. Labeling of the GFP channel is subtracted to facilitate visualization of the dTomato population. dTomato^{+} cells are visible in the region of the left habenula at 37 hpf (Time = 9:00:00).

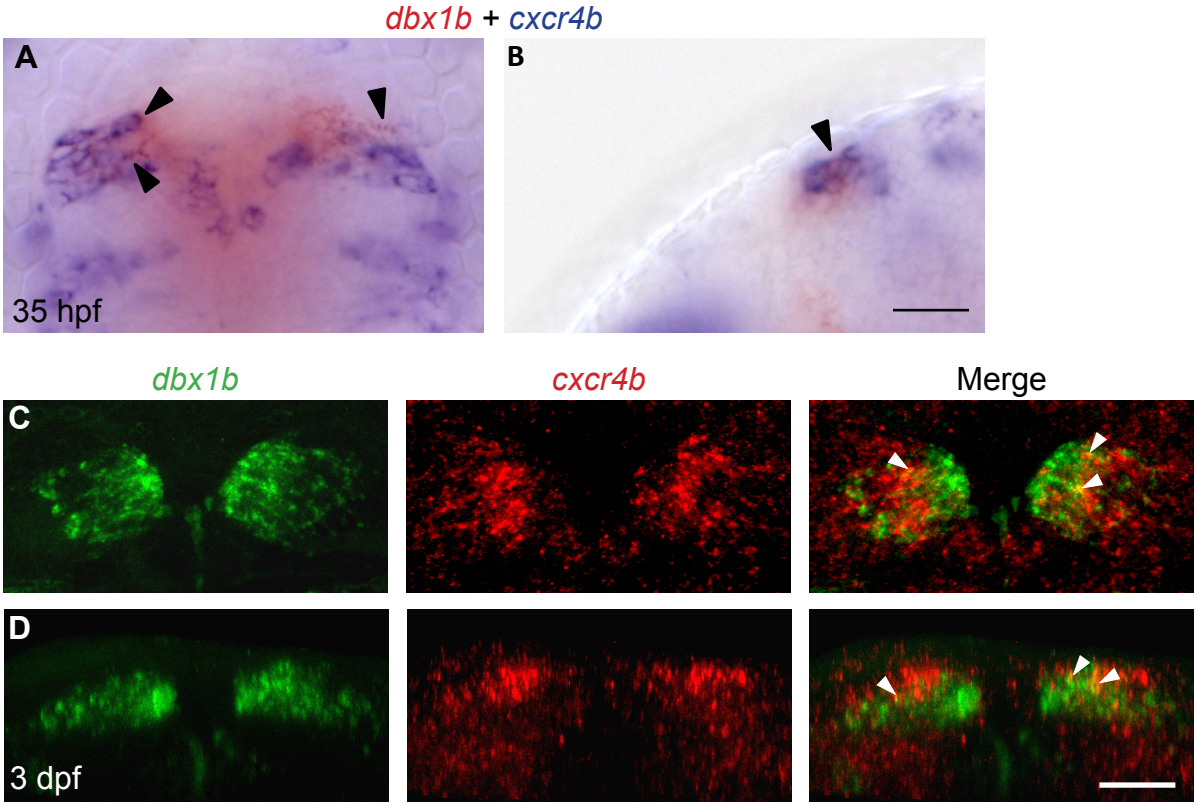

Fig. S1

Fig. S1: Partial overlap in *cxcr4b* and *dbx1b* expression.

Visualization of *dbx1b* and *cxcr4b* transcripts by (A,B) colormetric *in situ* hybridization at 35 hpf or by (C,D) fluorescent *in situ* hybridization at 3 dpf. (A,C) Dorsal (B) lateral and (D) frontal views show partial co-localization of transcripts in a subset of dHb cells (arrowheads). Scale bar, 30 μm.

TgBAC(dbx1b:nls-dTomato); *TgBAC(gng8:GFP-CAAX)*

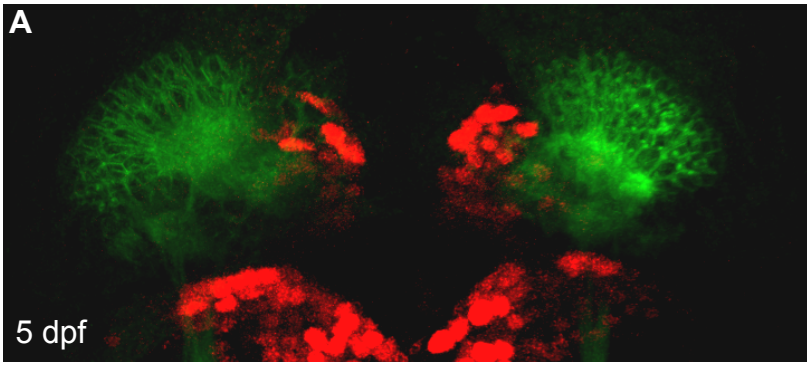

dbx1b Cre lineage tracing; *TgBAC(gng8:GFP-CAAX)*

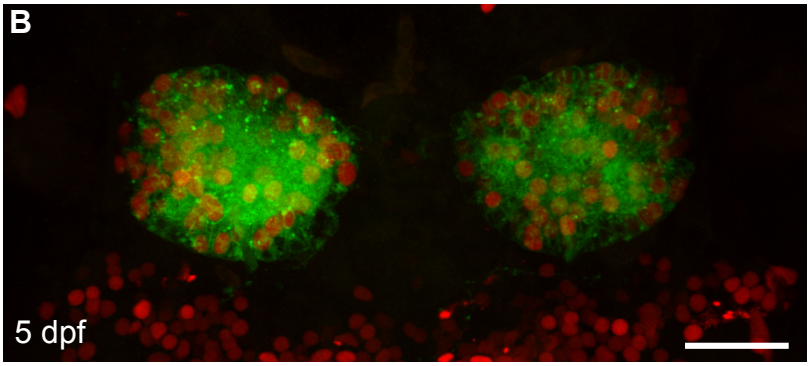

dbx1b Cre lineage tracing; *TgBAC(gng8:GFP-CAAX)*

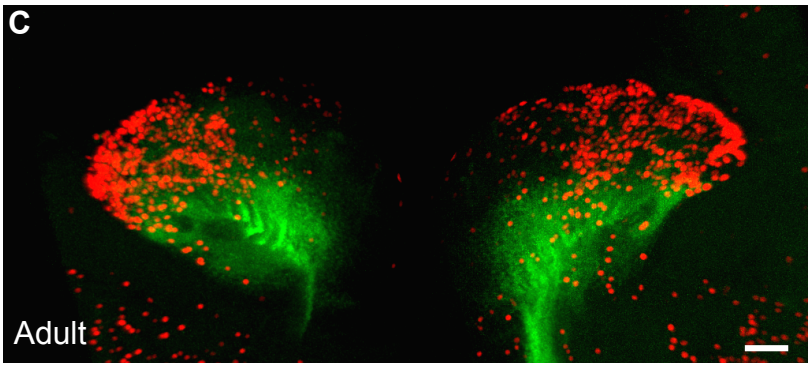

Fig. S2

Fig. S2: Medial *dbx1b*$^{+}$ cells give rise to all dHb neurons

TgBAC(gng8:CAAX-GFP) labels the cell membranes of dHb neurons (green). (A) *TgBAC(dbx1b:nls-dTomato)* labels cells medial and ventral to the GFP labeled neurons. Dorsal view, 5 dpf. (B,C) Lineage tracing using Cre recombinase under control of the *dbx1b* promoter [*TgBAC(dbx1b:Cre-mCherry)*] and a floxed reporter line [*Tg(β-actin:loxP-hmgb1-eCFP-loxP-H2B-mCherry)*] labels neurons throughout the dHb with nuclear mCherry at (B) 5 dpf and (C) in adult brain sections. Scale bars are (A,B) 30 μm and (C) 50 μm.

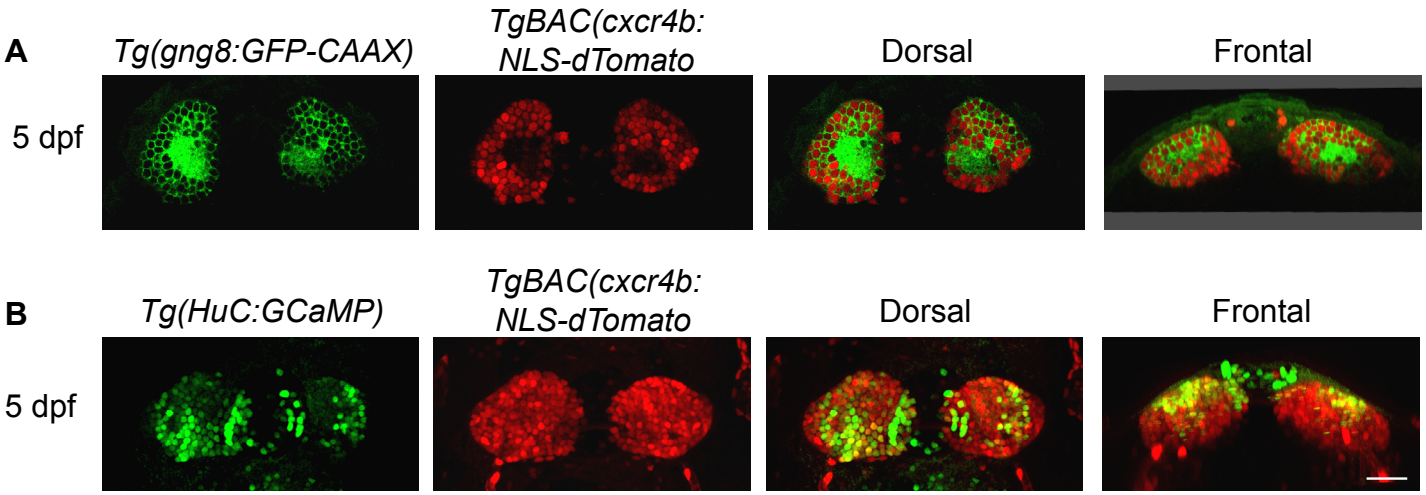

Fig. S3

Fig. S3: Persistence of fluorescent labeling in dHb neurons of transgenic larvae.

In 5 dpf *TgBAC(cxcr4b:nls-tdTomato)* larvae, dTomato labeling persists in dHb neurons distinguished by (A) *TgBAC(gng8:CAAX-GFP)* or (B) *Tg(HuC:H2B-GCaMP6s)* labeling. Scale bar is 30 μm.

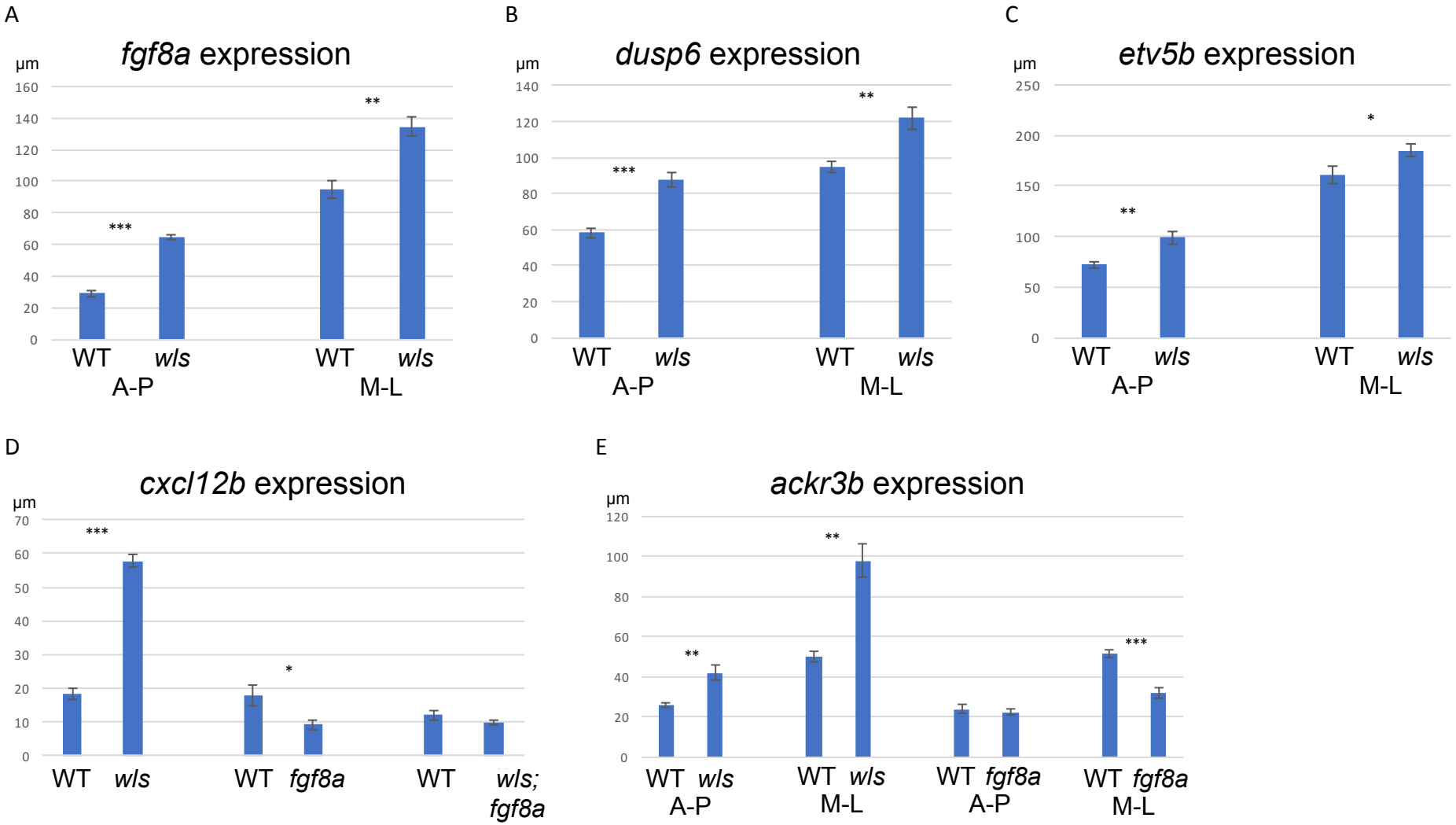

Fig. S4

Fig S4. Quantification of spatial domains of diencephalic gene expression.

Measurements (μM) of (A) *fgf8a*, (B) *dusp6,* (C) *etv5b*, (D) *cxcl12b* and (E) *ackr3b* gene expression domains in *wls*$^{-/-}$*, fgf8a*$^{-/-}$*,* and *wls*$^{-/-}$*; fgf8*$^{-/-}$ mutants and their WT siblings along the anterior-posterior (A-P) and medial-lateral (M-L) axes of the brain. Statistical analysis performed with Students t-test. * represents $p< 0.05$; ** $p< 0.0005$ and *** $p< 0.5 \times 10^{-5}$.

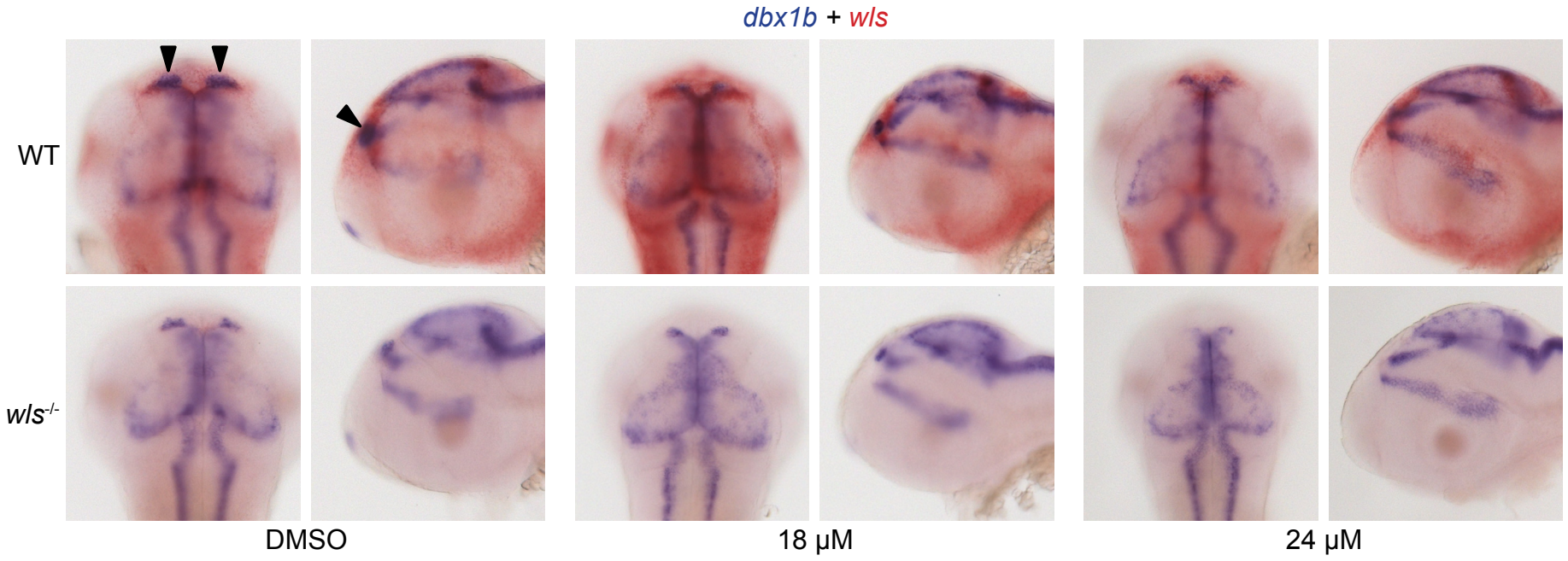

Fig. S5

Fig. S5: Inhibition of Fgf signaling reduces *dbx1b* and *cxcl12b* expression domains in a dose-dependent manner

Between 24 and 48 hpf, WT and *wls* mutant sibling embryos were treated with either 0.3% DMSO, 18 µM SU5402 + 0.3% DMSO, or 24 µM SU5402 + 0.3% DMSO. Diencephalic expression of *dbx1b* (arrowheads) is reduced in a dose-dependent manner in WT and *wls* mutants.

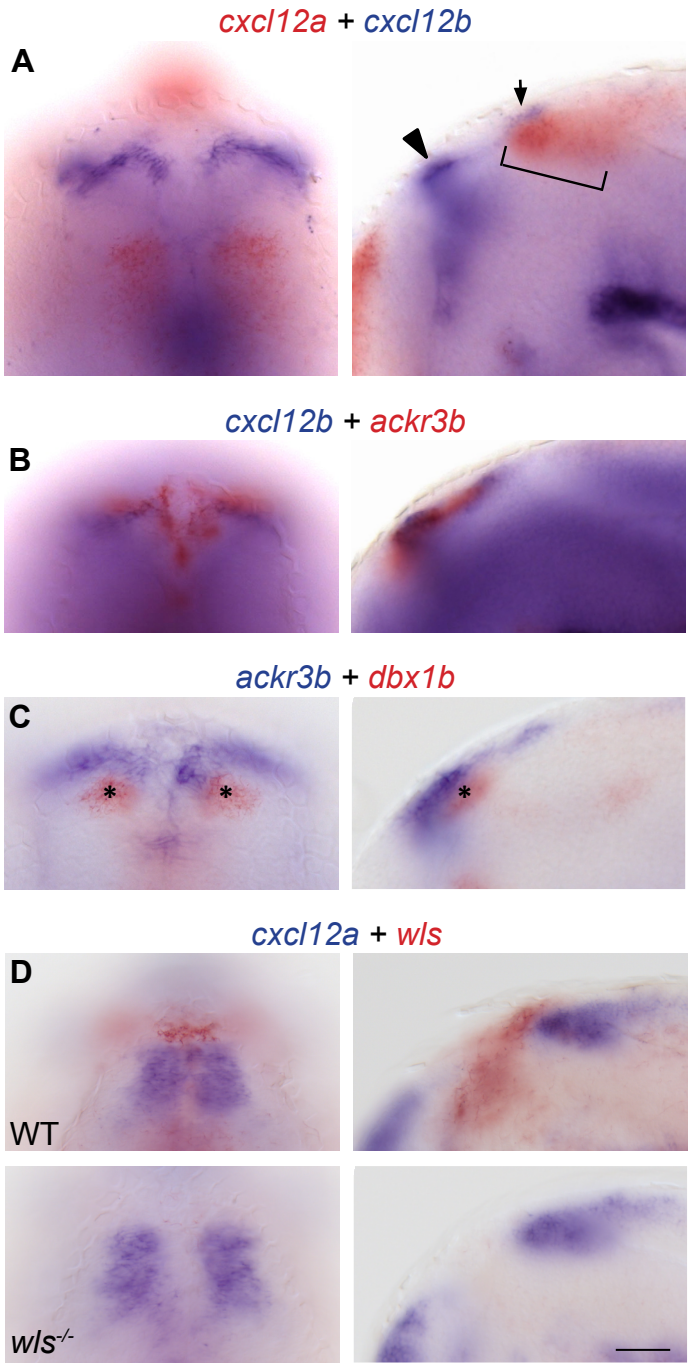

Fig. S6

Fig. S6: Diencephalic expression of genes in the Cxcr4-chemokine signaling pathway.

(A) The *cxcl12a* gene is expressed ventral and caudal (bracket) to the developing habenulae. *cxcl12b* transcripts are found in high levels rostral (arrowhead) and lower levels caudal (arrow) to the dHb. (B) Transcripts for *ackr3b* are found anterior and medial to the rostral domain of *cxcl12b* expression and (C) the *dbx1b*$^{+}$ progenitors (asterisks). (D) Expression of *cxcl12a* is not affected in *wls* mutants. Dorsal (left) and lateral (right) views. All embryos are 35 hpf. Scale bar is 50 μm.